Journal of Neonatal Surgery
ISSN(Online): 2226-0439
Vol. 14, Issue 16s (2025)
https://www.jneonatalsurg.com

OPEN ACCESS

Development and optimization of efinaconazole-loaded nanostructured lipid carriers: Enhanced antifungal efficacy and skin penetration for topical treatment of superficial fungal infections

Akshay Kumar[1], Ayushi Singh[2], Sunil Kumar[1,*3]

[1]School of Pharmaceutical Sciences, Om Sterling Global University, Hisar-125001, Haryana, India

[2]Invictus Oncology Pvt. Ltd., Delhi-110092, India

[3]Atam Institute of Pharmacy, Om Sterling Global University, Hisar-125001, Haryana, India

***Corresponding Author:**

Email: sunilkundu450@gmail.com

Cite this paper as: Akshay Kumar, Ayushi Singh, Sunil Kumar, (2025) Development and optimization of efinaconazole-loaded nanostructured lipid carriers: Enhanced antifungal efficacy and skin penetration for topical treatment of superficial fungal infections. *Journal of Neonatal Surgery*, 14 (16s), 843-866.

ABSTRACT

The broad-spectrum topical triazole antifungal agent efinaconazole (EFI) has poor bioavailability because it demonstrates limited water solubility combined with inadequate persistence and penetration through the skin. This research studied nanostructured lipid carriers containing efinaconazole (EFI-NLCs) for developing an evaluation of their characteristics and antifungal properties *in vitro* investigations. The researchers manufactured EFI-NLCs through high-pressure homogenization while evaluating their characteristics *via* PDI analysis, zeta potential measurement, EE% determination, SEM imaging, thermal analysis and FTIR spectroscopy evaluation. Scientists conducted tests for *in vitro* drug release as well as antifungal susceptibility assessment and cytotoxicity analysis. The research showed that EFI-NLCs contained nanosized dimensions together with distributed particles and possessed a desirable zeta potential complemented by encapsulation efficiency at 85%. SEM micrographs confirmed that the prepared nanoparticles exhibited spherical geometries with uniform distribution of their shapes. The FTIR spectrum indicated that EFI had no destructive chemical reactions with any of the excipients used. Drug diffusion from the NLC formulation showed a substantial rise based on drug release pattern analysis. EFI-NLC gels successfully passed stability tests which demonstrated maintained physical stability aspects at acceptable boundaries. These tests established low toxicity measurements together with superior antifungal properties against strains of *Candida albicans* and *Aspergillus* species. A software-based Central Composite Design (CCD) with Design-Expert enabled the optimization process for concentration of surfactant (%), concentration of total lipid (%) and time of homogenization (minutes). The optimization process used three response variables to find the best characteristics for the EFI-NLC formulation. The evaluation indicated that EFI-NLC gel shows encouraging qualities for treating superficial fungal skin infections topically.

Keywords: *Efinaconazole, Drug delivery, Central Composite Design, Cytotoxicity, Nanoformulations.*

1. INTRODUCTION

Public health battles a substantial fungal threat because these pathogens infect millions of individuals throughout the world annually. A wide range of diseases affect humans due to fungal infections which result in mucosal lesions and superficial skin along with extreme lethal mycoses [1,2]. Fungal infections happen within three defined categories including superficial and subcutaneous and systemic infections. The dermatophytes alongside yeasts and non-dermatophyte fungi cause superficial infections that frequently affect tropical, subtropical and temperate climate areas [2,3]. Dermatophytosis stands as the most widespread superficial fungal infection since it affects between 20–25% of global population numbers [4,5]. The four fungal genera which frequently cause infections in human beings include *Nannizzi, Microsporum, Epidermophyton* and *Trichophyton.* They primarily influence keratinized tissues like epidermis and other appendages as well as hairs and nails. The signs of dermatophytosis differ based on the infected body parts and the strength of the host immunity. The following diseases represent typical dermatophytosis manifestations: *Tinea capitis, Tinea cruris, Tinea corporis Tinea unguium* and *Tinea pedis* [4-6]. *Candida albicans* and other associated *Candida* species together with yeast types of genus are accountable for causing superficial fungal ailments. The symptoms of superficial candidiasis appear in various ways across the body including oral thrush and vaginal yeast infections and nail fungus and continual yeast skin infections [7]. Other than Candida species dermatomycosis can also be caused by *Fusarium aspergilluss copulariopsis* and *acremonium* which are different genera of non-dermatophytic molds [8–10]. Most fungal pathogens face an escalating clinical challenge from both intrinsic

and obtained antifungal resistance in modern medicine [11]. Medical experts use topical antifungal drugs as preferred drugs for treating superficial fungal infections. The pharmaceutical industry created efinaconazole as a 10 percent conventional solution during the development of new generation triazole topical antifungal drugs to address these issues. The therapeutic effectiveness of topical solutions depends on high drug concentration because they face reduced nail permeability which creates application issues. The drug solution has a high tendency to wash away from the nail surface following its application [12,13]. Clinical use of the medicine during an extended period results in allergic dermatitis and skin vesicles at the application site [14]. Most drugs encounter limited penetration through the stratum corneum skin layer because this layer functions as a filtration barrier to protect the skin tissue. Lipophilic properties of EFI moiety along with its low aqueous dissolvability rates seriously impair both skin permeability and biological availability of the drug [15,16]. The use of nanocarriers for improving drug transdermal delivery represents a new strategic promising approach to drug delivery systems with in recent years [17–19].The passive delivery method of nanocarriers represents an advanced drug delivery solution which operates more rapidly than traditional drug delivery systems [19]. Multiple forms of nanocarriers serve as active drug delivery methods for skin applications to boost permeability while targeting specific skin compartments [20,21]. The use of liposomes and solid lipid nanoparticles (SLNs) together with nanoemulsions, niosomes and nanostructured lipid carriers (NLCs) constitutes widespread utilization of lipidic nanoformulations for topical drug delivery systems [22–24]. Research on metal nanoparticles and polymeric nanoparticles in addition to nanospheres along with nanocrystals demonstrates potential for dermal and transdermal drug delivery use [25–28]. NLCs stand as advanced lipid nanoparticles in their second generation since they demonstrate potential to enhance delivery of antifungal medication EFI and other lipophilic drugs through their drug-delivery system capabilities. The composition of these lipidic nanoformulations (NPs) includes liquid and solid lipids which provide better drug loading ability and stability over the alternative delivery method employing solid lipid nanoparticles (SLNs). The drug penetration into stratum corneum receives increased support from nanostructured lipid carrier (NLCs) due to their low toxicity and enhanced nanoparticle characteristics [29–31]. Research shows that nanostructured lipid carriers (NLCs) demonstrate superior potential as nano-delivery systems than vesicular systems like liposomes and ethosomes regarding their drug-loading capabilities alongwith their ability to target skin organelles [32]. The purpose of this study aimed to build and optimize efinaconazole NLC dosage forms which could promote effective dermal delivery for treating fungi. Antifungal and release evaluation tests determined the effectiveness of the formulated product.

2. MATERIALS AND METHODS

Materials

Efinaconazole was provided by Chemvon Biotechnology Co. Ltd., China. Clotrimazole and luliconazole was obtained as a gift sample from Kusum Healthcare Pvt. Ltd., India. Glyceryl monostearate (GMS) was purchased from Central Drug house Pvt. Ltd., New Delhi. Compritol 888 ATO, Gelucire 48/16 Pellets, Propylene glycol monolaurate, Labrasol, Transcutol-P were obtained from Gattefosse India Pvt. Ltd., Mumbai, India, as a gift sample. Isopropyl myristate, Proylene glycol, PEG 400, Tween 80 and Span 80 were procured from Sigma Aldrich or Merck, Mumbai, India. Carbopol was provided from Lubrizol India Pvt. Ltd., Navi Mumbai, India. Distilled water was purified using double distilled water assembly. Tetrazolium salt (MTT) and Sabouraud dextrose agar (SDA) were purchased from Himedia Laboratories Pvt. Ltd., Thane, India. Human Skin cell (SK-Mel-1) was purchased from the National Centre for Cell, Pune, India. *Candida albicans* (ITCC 5480) and *Aspergillus* Species (ITCC 6538) were purchased from Indian Agricultural Research Institute (IARI), New Delhi, India.

Screening of components

Screening of solid lipids

The solubility determination of efinaconazole in various solid lipids (Compritol 888 ATO, Glyceryl Monostearate, Gelucire 48/16 Pellets) was performed by adding EFI in increments of 1 mg until it failed to dissolve further in the molten solid lipids (which were heated at 5ºC above their melting point). The amount of solid lipids required to solubilise EFI was calculated. The experiment was conducted in triplicate.

Screening of liquid lipids (oils) and surfactants

The solubility of EFI in various liquid lipids (Propylene glycol monolaurate, Labrasol, Isopropyl myristate, Transcutol-P, propylene glycol and PEG 400) and surfactants (Tween 80 and Span 80) was determined by adding excess amounts of drug in 3 ml of oils in small vials. The vials were tightly stoppered and were continuously stirred to reach equilibrium for 72 h at 25ºC in a mechanical shaker. After that, the mixtures were centrifuged using High Speed Centrifuge (3K30, SIGMA, Germany) at 5000 rpm for 30 min at about 25ºC. The supernatant was separated, dissolved in methanol and consequently, solubility was quantified by UV spectrophotometer at 210 nm.

Design for Formulation Trials

A Central Composite Design (CCD) was employed using Design-Expert software to statistically optimize the formulation parameters of efinaconazole-loaded nanostructured lipid carriers (NLCs) by evaluating the effects of total lipid concentration (%), surfactant concentration (%), and homogenization time (min) on entrapment efficiency (%), drug loading (%), and

particle size (nm). The experimental design included factorial, axial, and center points, with factors studied at five coded levels (-α, -1, 0, +1, +α) based on preliminary trials and literature. ANOVA was used to assess the significance of independent variables, and polynomial regression models were generated to predict responses. Contour Plots were utilized to visualize factor interactions, while the Desirability Function approach was applied to identify optimal formulation conditions by maximizing entrapment efficiency and drug loading while minimizing particle size. The optimized formulation was validated by comparing experimental and predicted values to confirm model adequacy shown in table 1.

Table 1. Coded levels independent variables and their corresponding levels for NLCs

Independent variable	Symbol	Coded levels				
		-α	-1	0	+1	+α
Total lipid concentration (%)	A	5.3	6	7	8	8.68
Surfactant concentration (%)	B	0.32	1	2	3	3.68
Homogenization time (min)	C	9.95	12	15	18	20.04

Preparation of NLC

NLC was formulated using solid lipid (glyceryl monostearate), liquid lipid (propylene glycol monolaurate) and surfactant (Polysorbate 80). The solid lipids were melted at a temperature range 5-10°C more than their melting point. Liquid lipid and the drug (efinaconazole) to be encapsulated were added to the melted lipids. An aqueous solution of surfactant(s) was heated to same temperature range as the melted lipids. Further, the lipid mixture was deluged into the hot aqueous solution having surfactant via magnetic stirrer (IKA RCT basic, India) for 30 minutes at 1200 rpm for preparation of primary emulsion. The resultant primary emulsion was transformed to the NLC through high-pressure homogenizer (IKA T25 digital Ultra Turrax, India) at 15000 RPM for 15 minutes, followed by 5 minutes of sonication by probe sonicator. The obtained NLC dispersion was cooled down to room temperature [33, 34].

Optimization and characterization of NLC

Organoleptic features

Visual and olfactory senses were employed for evaluating the organoleptic features of EFI-NLC. The appearance of test samples was evaluated for three characteristics combined with initial form and phase separation and coalescence evaluation under storage conditions. The color and odor were evaluated to check storage temperature effects on consistency while confirming no color or odor alterations occurred [52].

Drug identification in NLC by Mass spectrometry (MS)

After dissolving NLCs in methanol, the mixtures were sonicated for 10 minutes while performing intermittent shaking to obtain the encapsulated drug from the lipid structure. The solution was filtered through 0.45-micron PVDF filter for removing lipid particles after sonication. Mass spectrometry (Waters Corporation, Massachusetts, USA) follows drug analysis of the extracted substance. Drug ionization occurs through TOF MS or corresponding methods based on drug characteristics. During the ionization process, the device separated molecular ions through their m/z ratio until it detects a corresponding match with known reference spectra found in dedicated drug databases. The mass spectrometry technique delivers structural information to establish drug identification accuracy in complicated drug delivery vehicles including NLCs [58].

Particle size, PDI, and zeta potential evaluations

The particle size investigation of NLCs formulations was performed through photon correlation spectroscopy with Zetasizer (Malvern Instruments) as the measuring instrument. A PCS instrument calculates z-average particles size together with PDI which shows distribution width. The analysis of filtered double distilled water-diluted solutions occurred at 25°C and 90° scattering angle using Whatman filter papers [16, 33]. The experiments were performed three times for each measurement point and results showed mean values with standard deviation (SD) calculated from three readings.

Entrapment efficiency (EE) and drug-loading capacity

A gentle shaking procedure mixed both NLC dispersion and drug until the distribution reached homogeneity. A 1.0 ml portion of the dispersion submitted to centrifugation through a High-Speed centrifuge at 10,000 rpm for 30 minutes received dilution with 9.0 ml of methanol before separation of free drug from nanoparticles occurred. The researchers employed a

0.45µm Millipore membrane to eliminate all remaining particulate matter after subjecting the supernatant to filtration [36-37]. The analysis of free drug concentration in filtrate samples followed similar approach reported by Agarwal and research group [38]. Determination of the NLC-drug contents by subtracting the residual free drug from the initial drug added to the solution. Standard equations 1 and 2 were employed for the calculation of percent entrapment efficiency (EE%) and drug loading (DL%) by determining entrapped drug to total drug ratio for EE% while evaluating entrapped drug to NLC total weight ratio for DL%.

$$EE\% = \frac{W(Total)-W(Free)}{W(Total)} \times 100 \qquad 1$$

$$DL\% = \frac{W(Total)-W(Free)}{W(Lipid)} \times 100 \qquad 2$$

W_{free}, W_{lipids}, and W_{total} are analysed weight of drug in supernatant, weight of lipid added in system and the weight of drug added in system, respectively.

Scanning electron microscopy (SEM)

The EFI-NLC formulation placed at -80 °C for 24 hours before lyophilizing it using a instrument freeze-drier (Macflow Engineering Pvt. Ltd., India) to produce a dry powder. Evaluation of EFI-NLCs morphology occurred through scanning electron microscopy (JEOL Limited, Japan). The imaging procedure required a gold coating layer on the lyophilized sample to boost its conductivity levels. SEM analyzed the sample at 200,000× magnification with 5.0 kV acceleration voltage. The study used this technique to unveil extensive information about the EFI-NLC surface anatomy and design features [39].

FTIR Spectroscopy

The FT-IR spectra of pure efinaconazole along with its formulations through the use of FT-IR spectrophotometer (PerkinElmer, Inc, MA, USA). A sample weighing 2-5 mg was combined with 100 mg of potassium bromide (KBr) before subjecting it to grinding then pressing into a transparent pellet with a hydraulic press. Analysis of spectra ran from 4000–400 cm^{-1} using a settings resolution of 4 cm^{-1} per sample. IR spectroscopy analysis of obtained spectra helped detect functional groups present in Efinaconazole API and its excipients while identifying any potential bonds that formed between these substances through peak matching of pure efinaconazole, EFI-NLC Lyophilized formulation, GMS, Capryol 90, Polysorbate 80 and Carbopol 980 NF [40, 41].

Differential scanning calorimetry (DSC)

The crystal structure of EFI blended with lipid matrix was detected through differential scanning calorimetry analysis using instrument Perkin Elmer precisely (DSC 6000) Differential Scanning Calorimeter (PerkinElmer, Inc, MA, USA). DSC was used to record thermograms for crystallinity identification. Tight sealing procedures were used on standard aluminium pans which contained 1–5 mg weights of accurately measured free dried formulations. The thermal measurement process followed 10 °C/min while raising the temperature from 37°C to 400 °C. The reference system consisted of a blank pan. The measurements took place under inert conditions which relied on nitrogen purging [16, 33].

Characterization of EFI NLC gels

Physical Appearance

Physical examinations of the prepared gel included texture evaluations along with assessments of uniformity and clarity that were performed by visual and tactile methods. An evaluation of the texture was assessed both its smoothness along with its consistency before inspecting the uniformity across the sample area. The pureness of the solution was tested using light illumination to look for cloudiness. An assessment of the gel involved a review for foreign matter and contaminants to uphold quality measures and regulatory specifications [16, 42].

Viscosity and Torque measurement

The viscosity and torque testing of NLC samples were assessed using a Brookfield viscometer (Model: DV2T, extra viscometer, Brookfield Engineering Laboratories, USA) with spindle No. RV-06. The tests were performed at a precise temperature of 25 ± 0.5°C because this level was chosen to maintain testing uniformity. The spindle has been run at 5.0 rpm speed while the viscometer acquired the recorded readings for viscosity together with torque measurements. Sample equilibrium at the test temperature before measurement took place in order to reduce temperature-related variations. The analysis of each sample was performed three times to check the reliability and consistency of the obtained outcomes. Rheological properties of the developed formulations were evaluated through the collected viscosity data and torque results for assessing stability along with pharmaceutical and cosmetic suitability [33, 43].

Measurement of pH

The pH determination for EFI-NLC gel formulation used a calibrated pH analyzer. A solution containing 10% w/v of NLC-Gel required measurement of 1 g NLC-Gel that was dissolved in 10 ml distilled water. The assurance of accurate pH measurements required 4-5 minutes of incubation followed by an equilibrium period for the sample. The measurement of pH was done three times to confirm the accuracy and repeatability of collected data points. Laboratory assessments of the formulation measured its compatibility with both skin pH and its stability following analysis of obtained values [43, 44].

Spreadability

The gel formulations were allowed for spreadability test through glass plate assessment. A clean glass plate received a pre-drawn 1.0 cm diameter circle where 1.0 g of the gel was situated. Another glass plate was added on top of the gel for a consistent contact. The gel received a 500 g standard weight for 5 minutes on top of the upper glass plate before measurement. The researchers noted the diameter expansion of the gel because of its spreading action following the time period. The authors designed this test to evaluate how easily the gel applied to and how evenly it spread onto the skin or alternative application surfaces [45, 46].

Drug content

A 1.0 gm of prepared gel from the tube was measured before dissolving it into solution with efinaconazole content at about 10 mg. The solution received its final dilution of 50 ml by mixing methanol and water in a 80:20 volumetric ratio as diluent solution. The solution needed chromatographic analysis after passing through a 0.45µm PVDF filter. The analysis took place through HPLC Chromatography which measured at 210 nm wavelength. The authors used equation 3 to evaluate drug content in the analysis [44].

$$Drug\ content = \frac{Practical\ yield}{Theoretical\ yield} \times 100 \qquad 3$$

In vitro studies

Preparation of phosphate buffer saline (pH-7.4)

For the preparation of phosphate buffer saline solution, disodium hydrogen phosphate (2.38g), potassium dihydrogen phosphate (1.36g) and 8.0g of sodium chloride (8.0) were accurately weighed and dissolved in appropriate water to make 1000 ml. The pH 7.4 was adjusted with orthophosphoric acid (OPA) [47].

In vitro release study

Drug release assessments occurred through Franz diffusion apparatus from Logan Instruments Corp, India which employed cellulose acetate membranes. A continuous stir operated at 32 ± 0.5 °C within the receptor compartment which contained phosphate-buffered saline (PBS) pH 7.4 solutions with 10% ethanol. The membrane solution process involved PBS pH 7.4 soaking before it was installed as a barrier between donor and receptor sections. Each experiment used 500 mg of the active substances through 5 mg efinaconazole where the test group received EFI NLC Gel 1% while the control group received efinaconazole Conventional Gel 1% (Control). Under sink conditions the experiment sampled medium aliquots at 0.5, 1, 2, 4, 6 and 24 hours to replace them with new medium during the diffusion process. The determination of drug concentrations at 210 nm wavelength required UV spectroscopy following cumulative dilution correction calculations. The experiments took place three times with each sample [33].

In vitro cytotoxicity investigation

In vitro cytotoxicity test was allowed to analyze the toxic properties of excipients (employed in nanoparticle formulation) on human dermal cultures. Cytotoxic potential of EFI loaded NLC preparations was examined in SK-Mel-1 cell line through MTT (3-(4, 5-dimethyl thiazol-2yl)-2, 5-diphenyl tetrazolium bromide) assay method. Cytotoxic evaluation by using three comparative samples also included cells with lipidic nanoparticle-gel without EFI (control) and both cells with EFI and cells with lipidic nanoparticle-gel (test). The test group received evaluation across eight control groups which assessed 8 different concentrations from 6.17µg/ml up to 500µg/ml.

The cell suspensions at a density of 1 × 106 cells/ml were prepared by either extracting adherent cells with trypsin. The experiment utilized 0.1 milliliters of medium provided per well in 96-well plates using cell densities between 103 to 106 cells per milliliter per well. Each MTT assay consisted of three separate conditions including blank wells with medium only together with untreated control wells and test wells. The tested liquid solution was placed under incubation at 37 °C using 5% CO_2 during a 24-hour period before it was gently removed from each well. The cells received clean DMEM media containing 10% FBS after the exchange of each well. The 20 µl solution of MTT (5 mg/ml) was poured to the plates which were incubated for 2-3 hours under a 5% CO_2 atmosphere at 37 °C until purple formazan crystal appeared. Each well received 100 µl dimethyl sulfoxide (DMSO) solution to serve as the dissolving agent along with micropipette mixing that lasted 45 seconds before a 10-minute incubation at 37 °C. The optical density was examined at 595 nm using micro titer plate reader against the reference wavelength 655 nm while maintaining DMSO as the blank solution. The measurements resulted in

determining the IC50 value for viability inhibition at 50% through graphical analysis [43, 50].

Zone of inhibition assay

The cylinder plate technique was employed for examining *in vitro* antifungal potential. Five samples (clotrimazole gel, luliconazole gel, efinaconazole gel, efinaconazole NLC gel and control (NLC gel without efinaconazole) were analyzed against two fungal strains *Candida albicans* (ITCC 5480) and *Aspergillus sp.* (ITCC 6538) to examine antifungal potential. The Sabouraud dextrose media (Himedia, Mumbai, India) was employed for cultivating *Candida albicans* at 30 °C temperature for 24 hours while Sabouraud dextrose media was employed for cultivation of *Aspergillus Sp.* at 30ºC temperature for 48 hours. With aid of a sterile, hiculture collecting device, the spores were cultivated and then dispersed into 20 ml media followed by filteration *via* sterile gauze. Inoculated media (1ml) was mixed to Sabouraud dextrose agar (100 ml) at 37±1°C temperature. 10 ml of the inoculated media was placed into petri dish having solidified agar media. One well in the five different petri dish were boredand packed with 0.1 g each of clotrimazole gel 1%, luliconazole gel 1%, efinaconazole conventional gel 1%, efinaconazole NLC gel 1% and control (NLC gel without efinaconazole), respectively. The mean zone of inhibition diameter (cm) was noted and analyzed comparatively [43, 51].

Stability studies

A stability investigation of efinaconazole containing NLC-gel took place in agreement with ICH guidelines Q1A (R2) under accelerated (40±2◦C and 75±5%RH) and room temperature (25±2◦C and 60±5%RH) atmospheric environment for six months inside HMG µp Based stability chamber (HMG, India). The study evaluated the globule size distribution and drug content along with polydispersity index through three-month time points from the initial withdrawal at month 1 until month 6.

Statistical analysis

The researchers showed data results through three independent measurements averaged with standard deviation (SD) computation. A statistical examination with ANOVA served to detect differences among groups and the Tukey-Kramer post-hoc test provided specific results between groups. The research used a test statistic threshold at 0.05 to identify statistically important data. The researchers performed the statistical evaluations through GraphPad Prism 10.4.1 software. The results achieved high reliability because this method detected fluctuations both within individual experiments and between the groups. The research design included ANOVA with a subsequent application of Tukey-Kramer post-hoc testing to provide simultaneous group evaluation and verify significant group results. The applied statistical technique delivered a reliable investigation of experimental results that produced reliable data interpretation. Standard scientific protocols guided all statistical work to improve result reproducibility and verify the effectiveness of the formulated product [33, 55].

3. RESULTS AND DISCUSSION

Screening of components

The selection of excipients for the development of efinaconazole-loaded nanostructured lipid carriers (EFI-NLCs) was based on their pharmaceutical acceptability, non-irritant, non-sensitizing properties, and their classification under the GRAS (Generally Regarded as Safe) category. The mean and standard deviation (SD) values of the selected excipients are presented in Fig. 1. As per findings of solubility investigations; EFI presented maximal solubility in glyceryl monostearate (GMS) (173.33±4.16 mg/ml), propylene glycol monolaurate (12.62 ±0.10 mg/ml) and Tween 80 (8.16± 0.17 mg/ml). Thus, EFI-NLCs were formulated using GMS (solid lipid), propylene glycol monolaurate (liquid lipid) and Tween 80 (surfactant). On the basis of visual inspection of smear test, binary lipid phase was found to be selected in the ratio 5:5 w/w (solid: liquid lipid ratio) for developing NLC. Mittal and research group demonstrated that increased solubility was found to be responsible for enhanced drug entrapment efficiency, ensuring a stable system. Lipids with maximal solubility were chosen for optimized NLC formulation [38, 61].

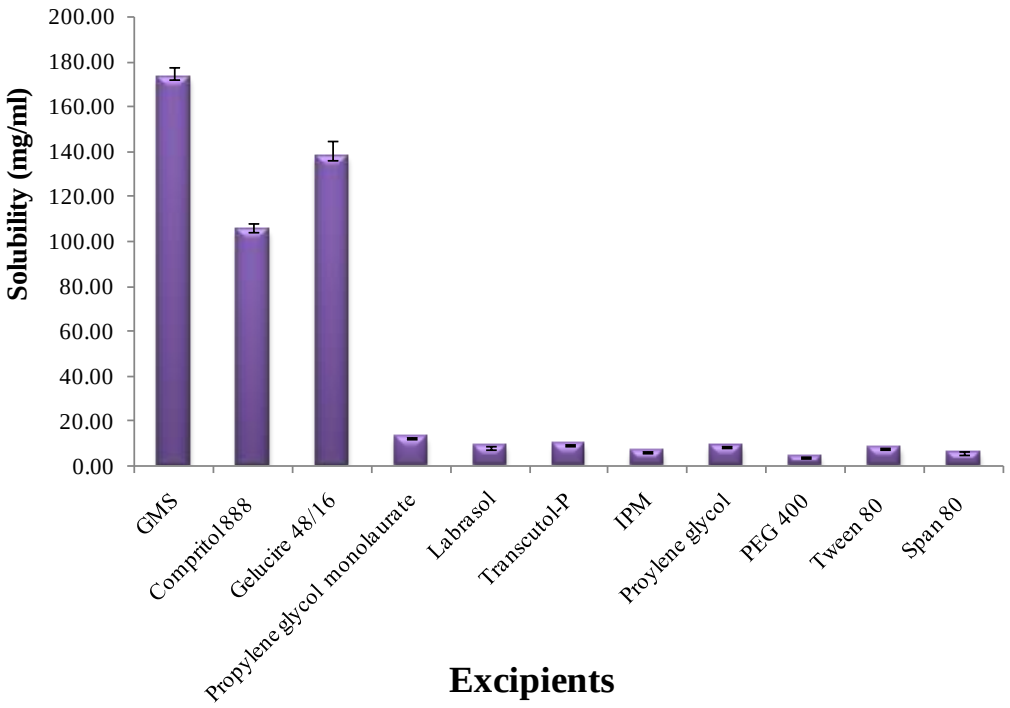

Fig. 1. Solubility of various excipients employed in NLC formulation.

Optimization of Formulation by QbD

The Central Composite Design (CCD) analysis successfully identified important process optimization information because it analyzed linear effects and interaction effects and quadratic effects of all factors. The employment of factorial points with axial and center points in the design framework enabled researchers to understand response surfaces thoroughly by delivering improved data precision when contrasted with full factorial techniques. The wider factor level range of CCD allowed researchers to gain better insight into complex non-linear responses by finding successful operating parameters. The efficient operation and adaptable nature of CCD enables strong management of processes through reduced experimental requirements resulting in both cost savings and time reductions and producing data that can be trusted [67].

Initial risk assessment

A 1.0% w/w drug concentration was used to prepare EFI-NLC at room temperature under 15 minutes of stirring at 15,000 rpm speed. The literature review produced results to determine multiple Critical Material Attributes (CMAs) and Critical Process Parameters (CPPs) that governed the formulation's performance. Total lipid concentration together with surfactant concentration and homogenization time (minutes) proved to be major contributors influencing the behavior of particle size along with drug loading and encapsulation efficacy. The research team utilized Design of Experiments (DoE) to determine the individual and combined effects between these factors and Critical Quality Attributes (CQAs). The analysis with Design of Experiments showed important correlations of these identified factors with Critical Quality Attributes because maintaining accurate lipid amounts and surfactant levels and controlling homogenization time are vital for formulation success. The selection of proper parameter settings proved essential for developing a formulation with correct and sizes alongside maximum drug volume and effective encapsulation. Researchers have obtained important knowledge that enables improved scale-up initiatives for EFI-NLC manufacturing and ensures reliable fungal management outcomes [68].

Design of experiment by 3-level Central Composite Design

For the optimization process utilized the Central Composite Design (CCD) for 3 crucial formulation variables including Total lipid concentration (%), surfactant concentration (%) and homogenization time (minutes). This optimization method worked to decrease particle size while simultaneously increasing entrapment efficiency and drug loading within the EFI-NLC formulation. The optimization method worked to find the optimal combinations between formulation elements to boost the complete fungal management capabilities of the formulation. Through Design-Expert® (Stat-Ease 360) software suggested conducting 20 experimental runs for examining variable effects on response factors. Each formulation was prepared following the experimental design parameters by adjusting the lipid and surfactant concentrations together with controlling homogenization time for specific trials. The study generated data concerning particle dimensions together with drug retention metrics and entrapment effectiveness that represented in Table 2. The data analysis revealed the most suitable

formulation parameters by locating best conditions for producing minimal NLC while maximizing both entrapment efficiency and drug substance loading levels as the main success criteria. The extensive formulation optimization research created a thorough view of critical quality attributes interactions from chosen formulation variables to establish a reliable fungal management EFI-NLC system [67, 70].

Table 2. Experimental design for NLCs with independent variables and experimental values of responses

Run	Total lipid concentration (%)	Surfactant concentration (%)	Homogenization time (minutes)	Response values		
				Entrapment efficiency (%)	Drug loading (%)	Particle size (nm)
1	6	1	18	66.4	2.21	149.33
2	7	2	9.95	76.12	7.98	229.34
3	8	3	18	76.93	9.75	203.88
4	8	3	12	74.9	6.19	300.99
5	8.68	2	15	79.31	12.77	226.87
6	5.32	2	15	70.57	8.86	144.48
7	8	1	12	81.21	11.32	308.49
8	7	2	15	85.99	13.84	142.88
9	7	2	15	84.55	13.32	143.08
10	7	2	20.04	74.39	7.32	130.69
11	6	3	18	76.93	10.98	241.82
12	7	2	15	85.75	13.75	142.88
13	7	0.32	15	71.32	5.73	228.58
14	6	1	12	67.92	4.98	165.68
15	8	1	18	75.8	10.42	153.92
16	6	3	12	74.44	9.38	205.86
17	7	2	15	84.89	13.7	142.72
18	7	2	15	85.19	14.1	138.06
19	7	3.68	15	75.94	8.56	304.25
20	7	2	15	84.95	13.4	141.356

Analysis of variance (ANOVA)

ANOVA served within Central Composite Design (CCD) to determine the model significance in assessing experimental data fit. Results of the analysis showed strong statistical significance together with an outstanding agreement with experimental observations thereby confirming the predictive capabilities and reliability of the designed method. The three experimental variables together with concentration of total lipid concentration (%), concentration of surfactant (%), and time of homogenization (minutes) proved influential for each observed outcome including particle size, encapsulation efficacy, and drug loading. A visual interpretation of response relationship dynamics between multiple factors appeared through 3D plots for surface response analysis after conducting the experiments. The response surface plots delivered enhanced visibility into how variable adjustments individually and jointly influenced the outcome measurement. The model quality along with significance was evaluated through F-values and R^2 values and p-values. The model explained a substantial amount of response variation based on the significant R^2 values. Statistical significance tests included F-values to analyze model effectiveness while p-values helped determine separate variable impacts [69]. The development of quadratic equations

allowed researchers to establish mathematical relationships between variables while model graphs generated from these equations provided an enhanced overview of the optimization process to improve EFI-NLC formulation development.

Entrapment efficiency (EE)

The EE (Response 1) across all 20 experimental runs ranged from 66.40 to 85.99%. Among the various ANOVA models tested, the quadratic model provided the best fit, with an R^2 value of 0.9946. The model was significant, as represented by an F-value of 103.88, meaning the model is highly relevant, and a p-value of <0.0001, confirming its statistical significant potential. The significant model terms include A, B, C, AC, BC, A^2, B^2 and C^2. Additionally, the Lack of Fit F-value of 1.56 has been suggested that the Lack of Fit is not significant, as shown in Table 3. The effect of the independent variables on EE is described by the coded quadratic equation:

$EE = 85.21 + 2.77\ A + 1.44\ B - 0.3895\ C - 2.78\ AB - 0.5438\ AC + 1.43\ BC - 3.56\ A^2 - 4.02\ B^2 - 3.45\ C^2$

Where, A-Total Lipid Concentration, B-Surfactant Concentration and C-Homogenization time

Table 3. Lack-of-fit (LOF) test for each experimental response (entrapment efficiency, drug loading and particle size)

Regression coefficients	Entrapment efficiency (%)	Drug loading (%)	Particle Size (nm)
Model	Quadratic	Quadratic	Quadratic
Intercept	85.21	13.69	141.79
A- Total Lipid Concentration	2.77***	1.22***	25.13***
B- Surfactant Concentration	1.44**	0.8882*	22.14**
C- Homogenization time (min)	-0.3895*	0.0278	-29.14*
AB	-2.78*	-2.37*	-11.28*
AC	-0.5438*	0.4788**	-33.91***
BC	1.43***	1.10***	13.72*
A^2	-3.56**	-1.03*	15.79**
B^2	-4.02**	-2.33*	44.34***
C^2	-3.45*	-2.15**	13.79***
R^2	0.9946	0.9957	0.9995
Adjusted R2	0.9897	0.9718	0.9891
Predicted R2	0.9686	0.9786	0.9889
F-value	103.88	156.85	230.54
p-value	<0.0001	<0.0001	<0.0001
Lack of fit F-value	1.56	1.35	0.7735

In coefficient of estimate, significance levels are indicated as follows: *** denotes a p-value less than 0.001, ** represents a p-value less than 0.01, and * indicates a p-value less than 0.05. Factors without any asterisk are considered not significant.

The coefficient estimate shows how much the response (EE) is expected to change with a one-unit change in a factor, while keeping all other factors at same levels. In an orthogonal design, the intercept has been presented the overall average EE for all the experimental runs. The coefficients then adjust this average on the basis of the specific settings of the factors, reflecting how each factor impacts the response. The equation with coded factors allows for predictions about the response based on specific factor levels. Typically, high levels are coded as +1 and low levels as -1. The observed coded equation is important for evaluating the relative effects of different factors on comparison with their coefficients.

The influence of different independent factors on Response 1 (EE) can be better understood through Contour model graphs. Fig. 2. illustrated these relationships, showing how these factors interact and contribute to the observed changes in EE. These visual aids provide a clearer understanding of how the model assumptions match with real data, as well as the individual and combined effects of the variables [33, 68].

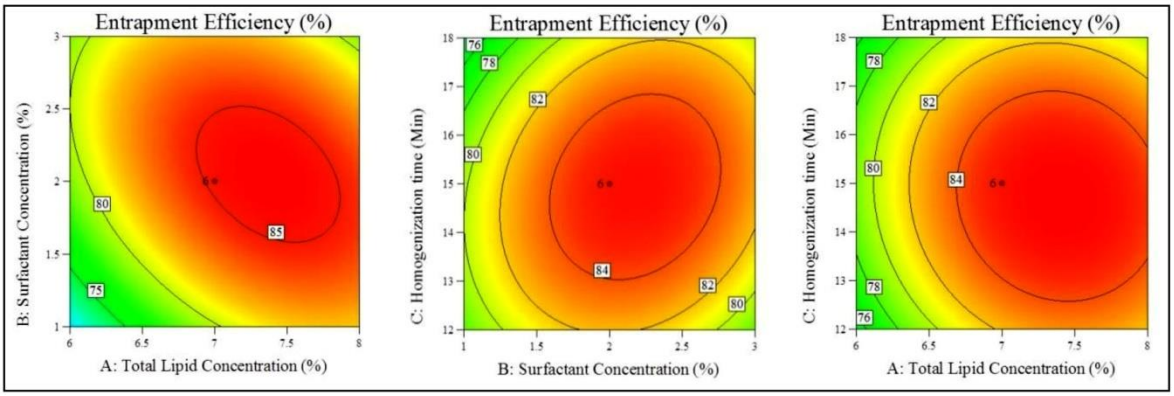

Fig. 2. Contour plot showing effects of different variables on EE (%) of efinaconazole.

Drug Loading (DL)

The DL (Response 2) across all 20 experimental runs ranged from 2.21 to 14.10%. Among the various ANOVA models tested, the quadratic model provided the best fit, with an R^2 value of 0.9957. The model was significant, as indicated by an F-value of 156.85, meaning the model is highly relevant, and a p-value of <0.0001, confirming its statistical remarkable potential. The significant model terms include A, B, C, AC, BC, A^2, B^2 and C^2. Additionally, the Lack of Fit F-value of 1.35 suggested that the Lack of Fit is not significant, as shown in

Table 3. The effect of the independent variables on DL is described by the coded quadratic

equation:

$$DL = 13.69 + 1.22\ A + 0.8882\ B + 0.0278\ C - 2.37\ AB + 0.4788\ AC + 1.10\ BC - 1.03\ A^2 - 2.33\ B^2 - 2.15\ C^2$$

Where, A-Total Lipid Concentration, B-Surfactant Concentration and C-Homogenization time

The coefficient estimate shows how much the response (DL) is expected to change with a one-unit change in a factor, while keeping all other factors at same levels. In an orthogonal design, the intercept has been presented the overall average EE for all the experimental runs. The coefficients then adjust this average on the basis of the specific settings of the factors, reflecting how each factor impacts the response. The equation with coded factors permits for predictions about the response on the basis of particular factor levels. Usually, low levels are coded as -1 and high levels are coded as +1. The obtained coded equation is important for evaluating the relative effects of different factors on comparison with their coefficients.

The influence of different independent factors on Response 2 (DL) can be better understood through Contour model graphs. Fig. 3. has been illustrated these relationships, showing how these factors interact and contribute to the observed changes in EE. These visual aids provide a clearer understanding of how the model assumptions match with real data, as well as the individual and combined effects of the variables [33, 67].

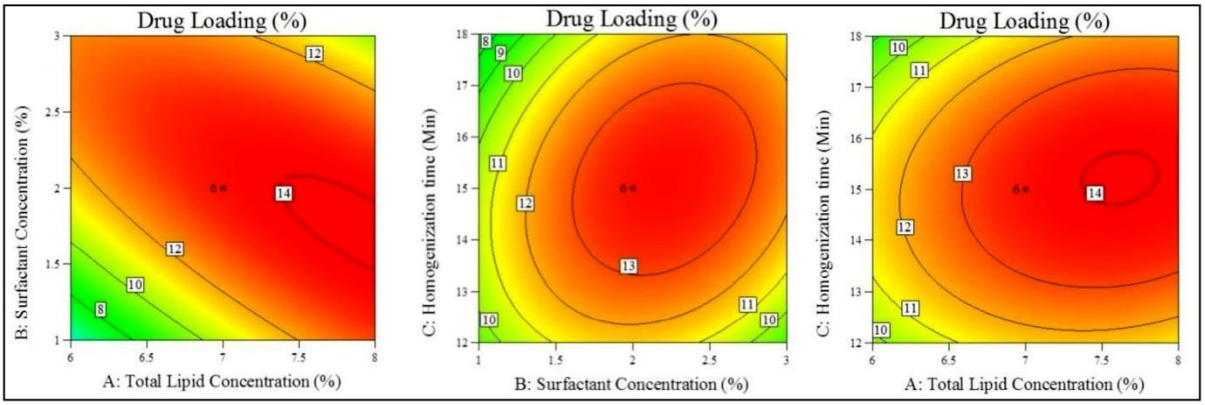

Fig. 3. Contour plot showing effects of different variables on DL(%) of efinaconazole.

Particle Size

The particle size response (Response 3) for all 20 runs ranged from 216.27 to 586.47 nm. These data were analyzed using various ANOVA models, with the quadratic model providing the best fit, showing an R^2 value of 0.9995. The model's F-value of 230.54 indicates its significance, meaning it fits the data well, while the p-value (<0.0001) confirms its statistical significance. Significant model terms include A, B, C, A^2, B^2, and C^2. The Lack of Fit F-value of 0.7735 suggests that the Lack of Fit is not significant as shown in Table 3. The effect of the independent variables on particle size is represented by the coded quadratic equation:

$$PS = 141.79 + 25.13\ A + 22.14\ B - 29.14\ C - 11.28\ AB - 33.91\ AC + 13.72\ BC + 15.79\ A^2 + 44.34\ B^2 + 13.79C^2$$

Where, A-Total Lipid Concentration, B-Surfactant Concentration and C-Homogenization time

The coefficient estimate shows how much the response (particle size) is expected to change with a one-unit change in a factor, while keeping all other factors at same levels. In an orthogonal design, the intercept has been represented the overall average particle size throughout all experimental runs. The coefficients then adjust this average on the basis of specific factor settings, showing how each factor influences the particle size.

This equation, employing coded factors, enables response predictions on the basis of particular factor levels. It is particularly useful for analyzing the comparative impact of each factor by assessing their coefficients, where low levels are coded as -1and high levels are coded as +1.

The influence of different independent factors on Response 3 (particle size) can be better understood through Contour model graphs. Fig. 4. illustrated the observed changes in particle size. These visual aids provide a clearer understanding of how the model assumptions match with real data, as well as the individual and combined effects of the variables.

The optimized NLC were required to qualify the criteria of achieving maximum entrapment efficiency and drug loading along with minimal particle size. The optimized nanoformulation was determined to have a total lipid concentration (%) of 7.207% w/v, concentration of surfactant (%) of 1.987% w/v, and a Homogenization time of 15.66 minutes. The predicted values for entrapment efficiency, drug loading and particle size were 85.337%, 13.812% and 140.097nm respectively. To validate this, trial experiments were conducted in triplicate under these conditions, and the experimental values of the dependent variables were compared with the predicted results. The observed encapsulation efficiency, drug loading and particle size were found 83.75±0.57, 14.24±0.43 and 139.9±4.9 respectively.

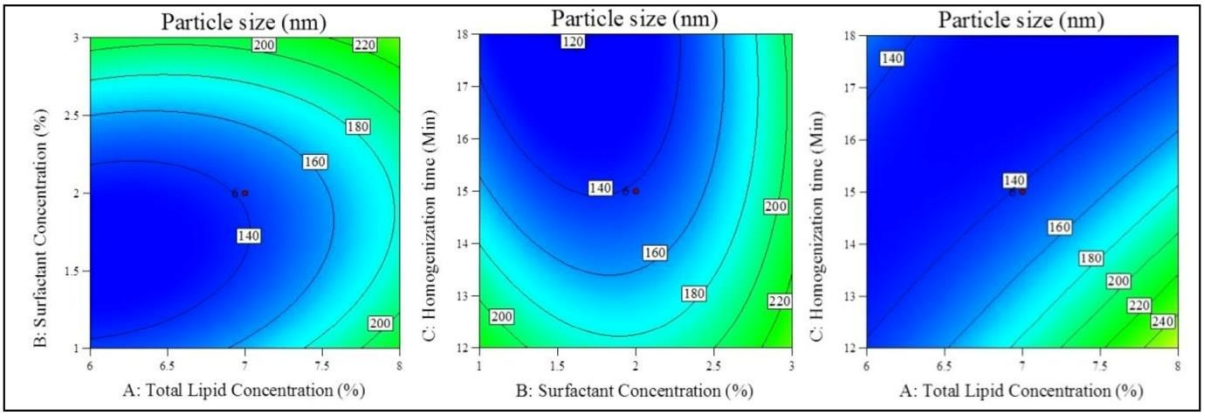

Fig. 4. Contour plot showing effects of different variables on particle size (nm) of efinaconazole.

The formulation (as described in Section Preparation of NLC) was then prepared and assessed for EE (%), DL (%) and particle size (Table 4). The observed values for particle size, PDI, and EE (%) were found to be approximately equal to the predicted values. This optimized nanocarrier (EFI-NLC) was used for further characterization and studies, confirming that the model provides the best fit. Most favorable conditions, experimental and anticipated values of response at optimized state are presented in table 4 [33, 70].

Table 4. Optimum conditions, experimental and predicted values of response at optimized condition

Optimum condition	Coded Levels	Actual Levels
Total lipid concentration (%)	0.207	7.207
Surfactant concentration (%)	-0.013	1.987

Homogenization time (min)	0.22	15.66
Response	**Predicted values**	**Experimental Values**
Entrapment efficiency (%)	85.337	83.75±0.57
Drug loading (%)	13.812	14.24±0.43
Particle size (nm)	140.097	139.9±4.9
	Desirability = 0.963	

$Z = Z_0 - Z_C / \Delta Z$

Where, Z and Z_0 were presented as coded and real levels of independent variables, respectively. ΔZ indicated step change while Z_C indicated actual value at central point.

Total Lipid Concentration = 7.207– 7 / 1 = 0.207

Surfactant Concentration = 1.987-2 /1 = -0.013

Homogenization time = 15.66 – 15 /3 = 0.22

If 2 Factors: A and B = AB graph

If 3 Factors: A, B and C = AB and BC, AC

If 4 factors: A, B, C and D = AB and CD, AC

Organoleptic features

The organoleptic features of EFI-NLC were examined by olfactory perception and visually. Regarding the appearance, there was no coalescence or phase separation and all samples retained their original appearance under storage conditions. It was evident that all of test samples had the same color and no particular odor, regardless of the storage temperature [52].

Drug identification in NLC by Mass spectrometry (MS)

The mass spectrometry analysis of the extracted drug from the nanostructured lipid carriers (NLCs) successfully confirmed the presence of the compound. The obtained molecular mass measurement resulted at 349.18 g/mol [59] while the documented value stands at 348.39 g/mol. An acceptable margin of 0.79 g/mol exists between the experimental measurement and the reported 348.39 g/mol and this variation stems from various experimental factors including ionization efficiency or instrumental calibration based on fig. 5. An analytical confirmation of the drug occurred through database comparison of the obtained mass spectrum. The coupling of MS analysis allowed to obtain structural information about the drug by verifying its composition remained unchanged throughout the intricate NLC formulation process. The reliability of using mass spectrometry to identify drugs in complicated nanoparticle systems has been established through these results [58, 62].

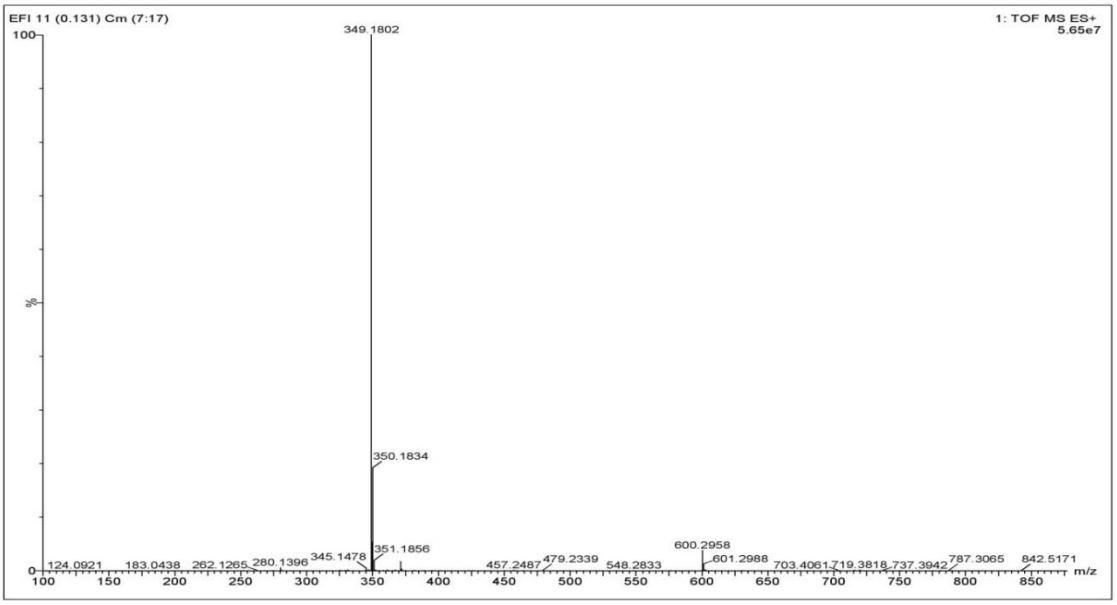

Fig. 5. Identification of the efinaconazole in NLC matrix by MS.

Particle size, PDI, and zeta potential

Analysis of particle size demonstrated that majority of NLCs existed between 80–200 nm since these systems needed prolonged processing duration along with high mechanical forces to generate tiny particles. The polydispersity index (PDI) values between 0.10 and 0.50 showed uniform size distribution which indicates a single size distribution and a PDI below 0.30 confirmed the homogeneous nature of nanoparticles thus reducing chances of aggregation. Nanoparticles exhibited stable characteristics based on their zeta potential range between −10.0 to −30.0. NLCs with a negative surface charge provided electrostatic repulsion forces that stopped particles from clumping up which enhanced the formulation's stability level. The specified characteristics serve as important requirements for drug delivery and extended retention. The optimized EFI-NLC preparation exhibited particles with favorable dimensions that meet pharmaceutical requirements based on Table 5 and Fig. 6. Garg and research group prepared NLCs which exhibited uniform particle size distribution with a low PDI, indicating homogeneity. The zeta potential ensured stability by preventing nanoparticle aggregation through electrostatic repulsion [39,53]. The outcomes have been showed that this developed formulation provides stable uniform features suitable for pharmaceutical drug delivery applications.

Table 5. Particle size, PDI and zeta potential of EFI-NLC

Formulation	Particle size (nm)	PDI	Zeta potential (mv)
EFI-NLC	139.9	0.289	-14.4

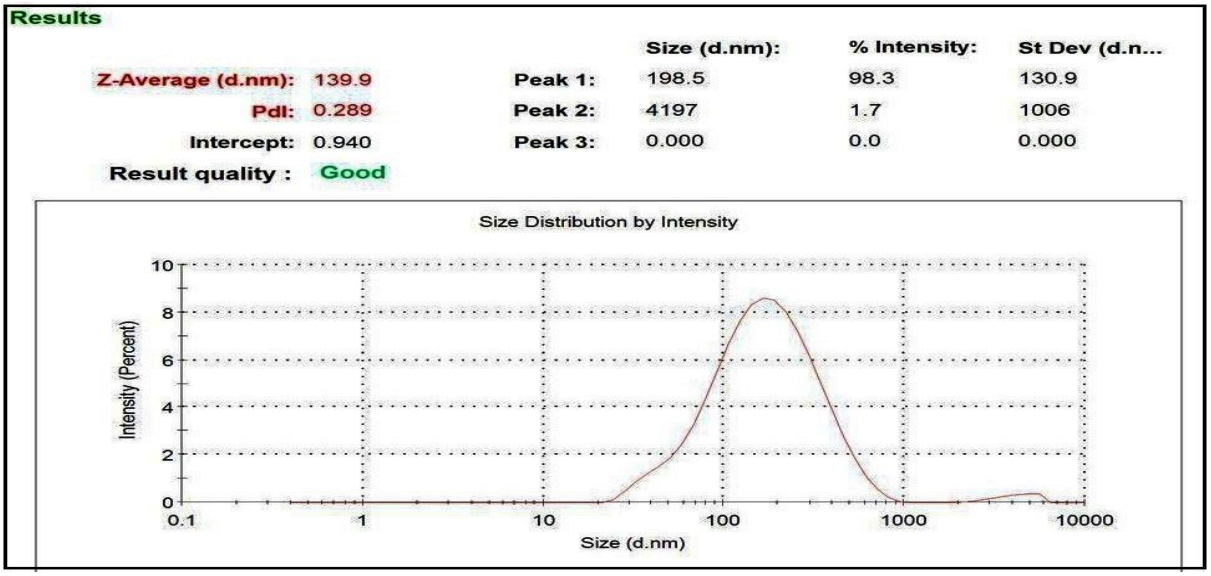

Fig. 6. Particle size and PDI of the optimized EFI-NLC.

Entrapment efficiency (%) and drug loading (%)

An optimal EFI-NLC displayed EE and DL values of 83.75±0.57 and 14.24±0.43 because of its distinctive NLC matrix structure. The solid lipid matrix component in NLC surrounds small areas containing highly drug-absorbent oil sections to boost drug holding capacity. The liquid lipids present in NLCs influenced EE significantly since they produce defects in crystal order which creates enough space for drugs to be incorporated successfully [33, 54].

Scanning electron microscopy (SEM)

The SEM photomicrograph showed NLCs formed spherical shapes with smooth surfaces that indicated their uniform morphology. The drying process probably led to occasional clumps because of dispersion medium concentration along with possible shrinkage effects. The experimental parameters related to drying techniques along with dispersion medium concentration demonstrated substantial effects on NLC uniformity together with stability. Consistent particle distribution together with aggregation minimization relies on optimal processing conditions. The spherical shape features with smooth exterior surface of NLCs helps them store drugs efficiently and control their release for pharmaceutical applications. The observations of clumped spherical structures indicated that accurate formulation optimizations should be implemented because instability formation occurs at present. Results demonstrated that optimizing processing conditions served as

essential to stabilize NLCs and enhanced formulation quality according to data shown in Fig. 7. which supported NLCs as suitable drug delivery systems. Similarly, in another study, SEM images displayed mainly spherical nanoparticles with uniform shape, closely resembling DLS results despite size variations due to measurement methods and factors [55].

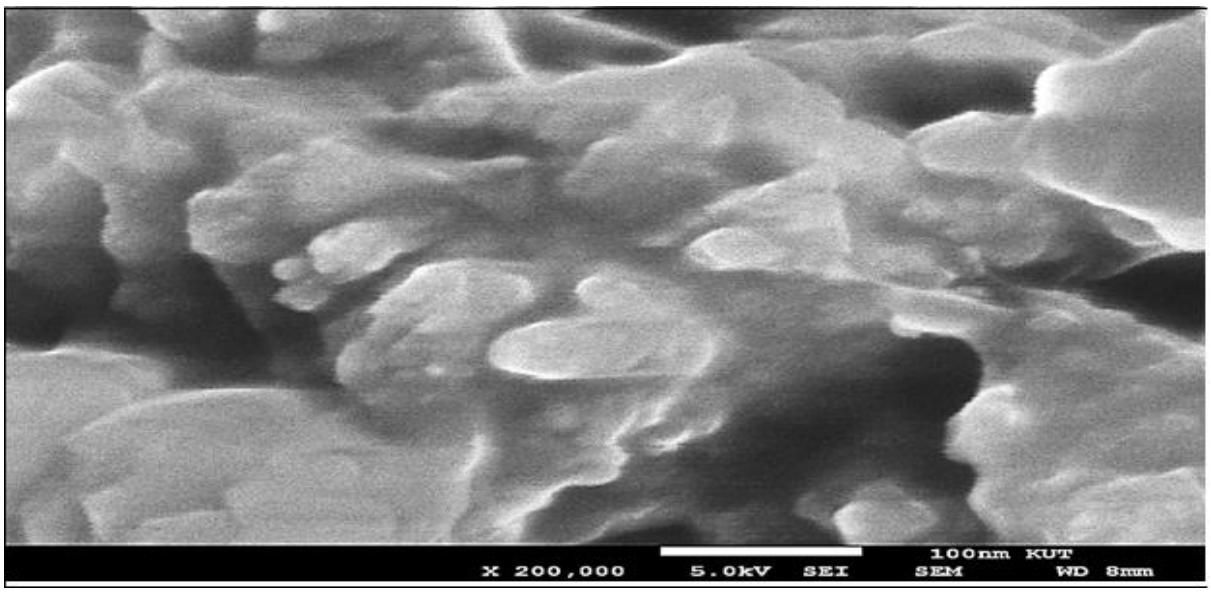

Fig. 7. Morphological characterization of NLC formulation using SEM

FT-IR spectroscopy

The pure efinaconazole FTIR spectrum showed specific peaks at 3325 cm^{-1} (O-H stretching) and 3085 cm^{-1} (aromatic C-H stretching) and 1635 cm^{-1} (C=C stretching) and 1270 cm^{-1} (C-O stretching). These peaks indicated hydroxyl groups and aromatic structures as well as an ether group. Aggarwal and group obtained similar spectrum of this drug as mentioned spectra herein [63]. Through IR spectroscopy of Polysorbate 80, Capryol 90, Carbopol 980 NF and GMS the EFI-NLC-LYO formulation showed minimal peak shifts together with quantitative changes. The O-H stretching peak showed increased width from 3300 to 3350 cm^{-1} which indicated that efinaconazole forms hydrogen bonds with excipients. The preservation of the 1720 cm^{-1} C=O stretching peak coming from Capryol 90 and GMS lipids confirmed the successful addition of excipients without substantial chemical modifications. The characteristic peaks from the pure drug clearly exist within the lyophilized formulation which confirmed that efinaconazole maintains its chemical stability after the formulation process along with its successful integration into the NLC system showed in fig. 8 by maintaining drug structural fidelity and demonstrating spectral stability tests.

Differential Scanning Calorimetry (DSC) Analysis

The DSC analysis (Fig. 9.) of pure efinaconazole represented a sharp endothermic peak at 87.47°C which had onset at 84.45°C and endpoint at 89.20°C matching the crystalline melting point of the drug with ΔH of 204.65 J/g. A highly crystalline structure showed itself through this particular pointed and clear peak. The EFI NLC LYO temperature scan revealed a less pronounced and wider thermal peak at 122.61°C that started at 115.91°C and ended at 125.63°C and had a minimal enthalpy change of 35.49 J/g. The shift to a higher temperature point combined with lower enthalpy signals a structural transition of the drug substance from crystalline state to either amorphous or partially disordered phase. The NLC formulation showed no peak indicating the original drug when measured by differential scanning calorimetry since it suggests drug molecules successfully embedded in the lipids.

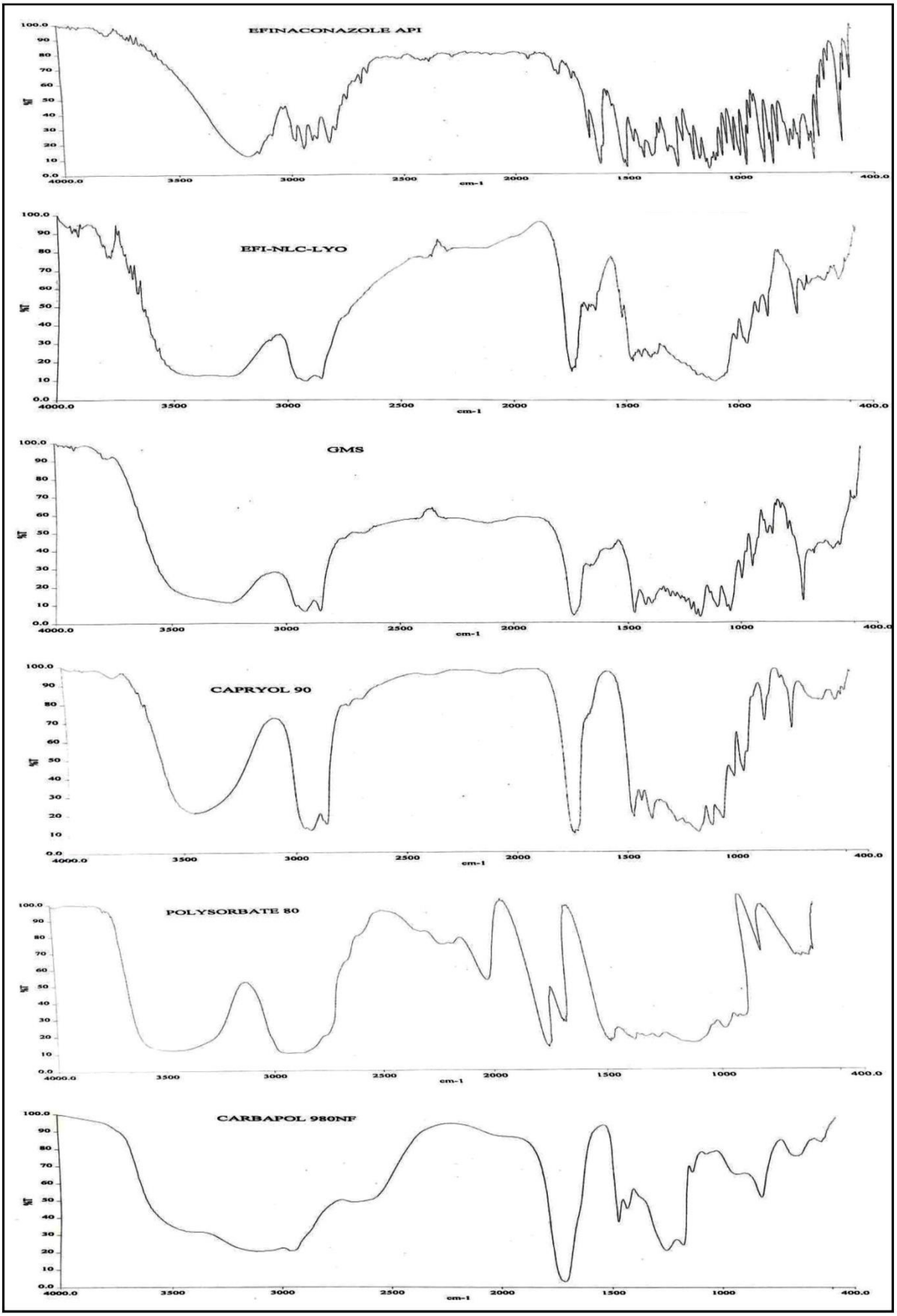

Fig. 8. FT-IR spectra of Efinaconazole API, EFI-NLC-Lyo, GMS, Capryol 90, Polysorbate 80 and carbopol 980NF.

Benefits occur when developing these structures because the reduction of crystalline areas leads to better drug accessibility. Fig. 9. demonstrated that efinaconazole physical state modification during formulation supports promised qualities of the nanostructured lipid carrier (NLC) delivery system. Agrawal and research group carried out the DSC analysis to confirm no drug-excipient interaction, showing EFI crystalline-to-amorphous conversion with a slight endothermic peak shift after encapsulation [43].

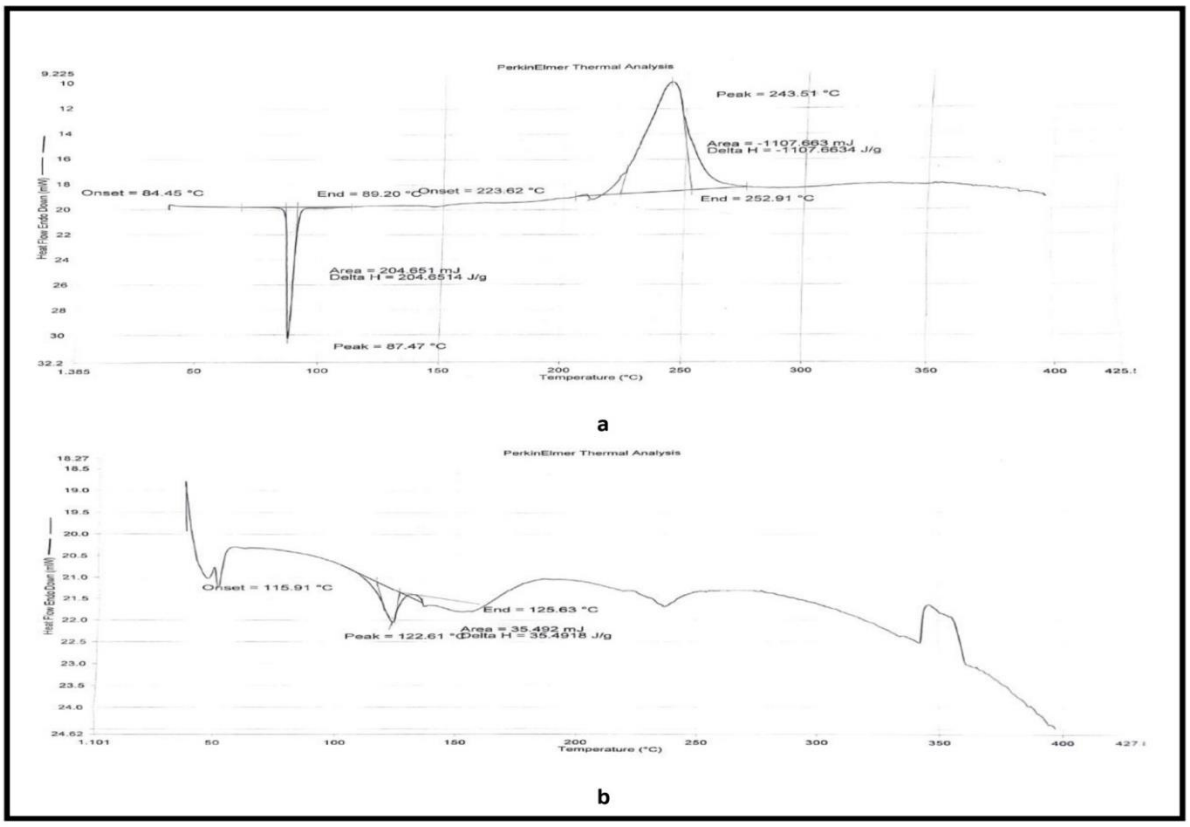

Fig. 9. DSC Thermogram (a) Efinaconazole API and (b) EFI-NLC-Lyo.

Characterization of EFI NLC gels

Physical Appearance

An evaluation of efinaconazole NLC gel involved testing its physical qualities which included its visual look as well as texture features plus uniformity and clarity. The gel appeared as white and smooth with homogeneous qualities and demonstrated semisolid consistency. The study using texture analysis demonstrated that the formulation had a smooth texture which provided easy usability for applications. Visual along with tactile tests ensured uniform distribution of the gel components by revealing its complete homogeneity. The examination of the clarity against a light source did not detect any turbidity which demonstrated the absence of phase separation. The assessment for foreign elements and contaminants of the formulation ensured compliance with quality standards. The results demonstrate the success of developing a properly designed NLC gel that exhibits attractive physical characteristics [42].

Viscosity and Torque

The Brookfield viscometer is used to obtain results for three gel formulations which showed their respective torque values and viscosities on Table 6. Studies revealed the placebo gel had 40,900 ± 4800 cps viscosity and 21.6 ± 3.3% torque which showed it had low flow resistance while maintaining moderate consistency properties. The conventional gel surpassed the placebo gel with its viscosity measurement of 70,300 ± 2600 cps and torque measurement at 38.7 ± 1.8% because gelling agents contributed to forming a more durable structure. The optimized EFI-NLC gel with its highest measured viscosity of 86,600 ± 3000 cps together with a torque reading of 43.3 ± 2.3% showed the best capability against flow resistance. Viscosity rises when lipid nanocarriers enter the formulation because they help manage drug release while also improving skin retention and formulation stability which makes them suitable for sustained drug delivery applications [43].

Table 6. Viscosity and torque of gel formulations

S. No.	Formulation	Viscosity (cps)±SD	Torque (%)±SD
1	Placebo Gel	40,900 ± 4800	21.6± 3.3
2	Conventional Gel	70,300 ± 2600	38.7± 1.8
3	Optimized EFI-NLC Gel	86,600 ± 3000	43.3 ± 2.3

Spreadability

The assessment of gel spreadability occurred through the glass plate method which involved applying 0.5 g of each gel into a 1 cm diameter circle followed by applying 500 g of weight for 5 minutes. A recording was made to determine the diameter growth caused by the spreading process. A placebo gel demonstrated maximum spreadability because its diameter expanded to 5.18 ± 0.53 cm which supports easy application of the medication. The spreadability of efinaconazole conventional gel 1% reached a moderate value of 3.33 ± 0.32 cm indicating that it was well suited for daily application. The optimized EFI-NLC Gel 1% demonstrated the lowest spreadability value of 2.92 ± 0.25 cm due to its high viscosity characteristic in table 7. The NLC EFI gel achievement showed better retention capabilities combined with controlled drug delivery despite having lower spreadability compared to other formulations. Khot and research group prepared NLC-based gel ensuring smoother application and improved drug delivery [64].

Table 7. pH and spreadability of gel formulations

S.No.	Formulation	pH ± SD	Spreadability (cm) ± SD
1	Placebo Gel	6.61±0.04	5.18 ±0.53
2	Conventional Gel	6.75±0.02	3.33 ±0.32
3	Optimized EFI-NLC Gel	6.82±0.03	2.92 ±0.25

Measurement of pH

A pH analyzer with calibration ensured the effective assessment of EFI-NLC gel formulation compatibility for skin environment because its pH value matched with human skin conditions. The dissociation process required 4–5 minutes for the solutions containing 1 g of different gels in 10 ml distilled water. The experiment measured pH values three times to guaranty the accuracy and reliability and reproducibility of recorded data. The obtained analysis demonstrated that the placebo gel exhibited a pH value of 6.61±0.04 and the conventional EFI gel maintained a pH value of 6.75±0.02 while the EFI-NLC gel showed a comparable pH value of 6.82±0.03 (as shown in table 7). The pH value of fabricated EFI-NLC gel fell within safe parameters for dermal use which ensured less skin irritation and better compatibility with skin tissue. Experiment results demonstrated that the formulation can be used for secure and effective topical application [33].

Drug Content

The HPLC analysis (at 210 nm) used filtered solution that contained 10 mg of efinaconazole per 1 g of gel which dissolved in a 80:20 v/v methanol-water mixture to 50 ml before passing through a 0.45 µm PVDF filter for removing particulate matter [66]. The analysis conducted in three repetitions demonstrated that efinaconazole remained at 100.12% ± 0.45 of its theoretical concentration thus proving both complete dissolution and exact formulation of the main component. The analysis established the effective incorporation and stability of benzyl alcohol preservative since its tested concentration matched the expected value of 99% ± 0.25%. The correct development of the gel together with excellent stability and precise concentration measurements for the drug material along with the preservative demonstrated the high-quality nature of the formulation [65].

In vitro release study

The Franz diffusion apparatus with a cellulose membrane evaluated drug release of efinaconazole gels through an NLC gel that maintained a longer drug release pattern than standard gel formulations. The NLC gel maintained higher drug release percentages than conventional gel during all time points starting from 0.5 and 1 hour up until 3, 6, and 24 hours of testing [66]. The 24-hour measurements showed that capacity of efinaconazole NLC gel to release 87.16±3.47% exceeded the 57.69±2.40% measured for conventional gel as depicted in Fig. 10. Formation of a nanostructured lipid carrier system within the NLC gel was found to enhance drug solubility, permeability and drug retention for improved membrane diffusion leading

to greater permeation rates. A sustained drug release pattern developed with time because of how the NLC delivery system controlled drug release. The drug release findings demonstrated significant differences (p<0.05) which were validated through Tukey's multiple comparisons test and establish NLC formulations as promising drug delivery methods. The outcomes demonstrated that efinaconazole gel formulated with NLC showed remarkable drug release properties which established it as a promising topical antifungal therapeutic.

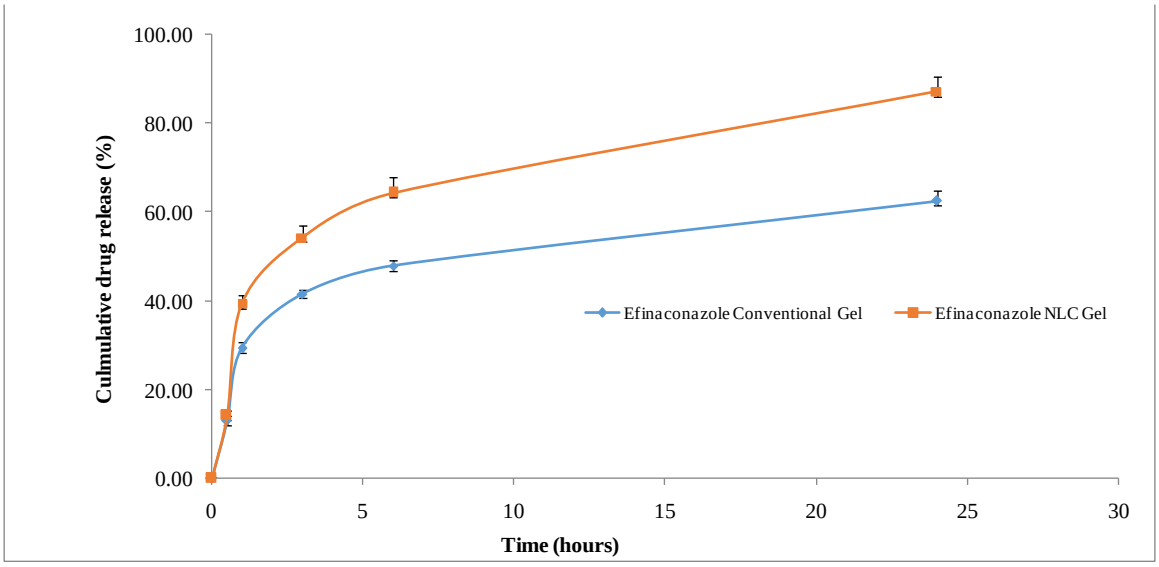

Fig. 10. *In vitro* drug release of efinaconazole conventional gel and EFI-NLC gel.

In vitro cytotoxicity and cell viability assay

Eight EFI-NLC samples underwent *in vitro* cytotoxicity testing through various concentration levels starting from 7.8µg/ml upto 500µg/ml. At 500 µg/ml concentration the EFI-NLC gel produced 62.36 ± 2.80% viable cells combined with 37.64 ± 2.80% dead cells. All data regarding cellular toxicity as a function of concentration for each tested group appears in Fig. 11. The results presented that every component used in efinaconazole-based NLC showed no indication of toxicity toward tissue. The data indicated that the formulated drug showed safety levels for topical application thus it demonstrates promise as a treatment component [38,60].

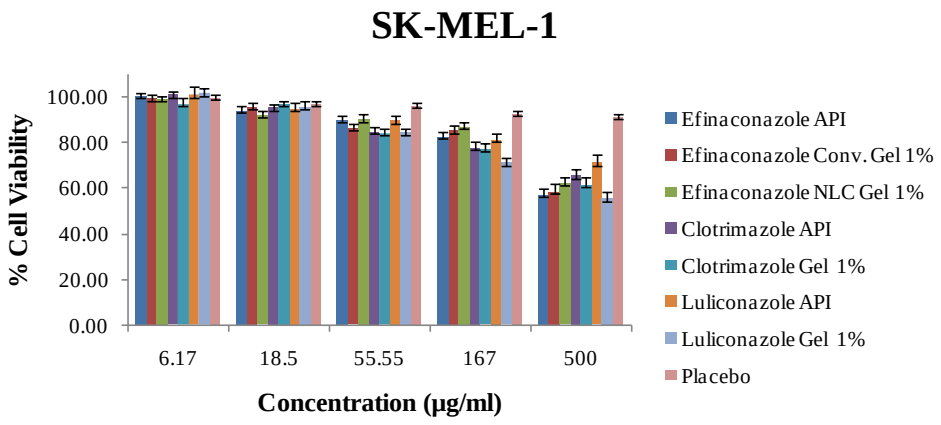

Fig. 11. Comparative *in vitro* cytotoxicity and viability data of all groups.

In vitro antifungal study

The antifungal potential for clotrimazole gel 1%, luliconazole gel 1%, efinaconazole conventional gel 1%, efinaconazole NLC gel 1% and control (NLC gel without efinaconazole) against the *Candida albicans* and *Aspergillus Sp.* is presented in Fig. 12. The mean zone of inhibition diameter for clotrimazole gel 1%, luliconazole gel 1%, efinaconazole conventional gel

1%, efinaconazole NLC gel 1% and control (NLC gel without efinaconazole) was observed against *Candida albicans* was 2.52±0.02 cm, 3.22±0.02 cm, 4.54±0.04, 4.95±0.04 cm and no inhibition showed in control, respectively and for the same against *Aspergillus Sp.* was 3.06±0.06 cm, 5.39±0.41 cm, 5.45±0.06 cm, 5.91±0.02 cm and 1.85±0.05 cm, respectively. The statistical investigation (Dennett's and Turkey's multiple comparison test) was employed between formulation versus control sample formulations and the *p* value was observed to be <0.0001 for all samples confirming valuable difference with respect to control formulation. Further, from the findings, the antifungal activity assessment demonstrated that the efinaconazole loaded NLC gel (1%) exhibited the highest zone of inhibition against both *Candida albicans* (4.95 ± 0.012 cm) and *Aspergillus sp.* (5.89 ± 0.017 cm) compared to other tested formulations. Antifungal effectiveness tests demonstrated that the conventional efinaconazole gel, clotrimazole gel and luliconazole gel demonstrated noteworthy antifungal properties although luliconazole exhibited stronger activity than clotrimazole. Plotting the control NLC gel without efinaconazole revealed no inhibitory effects against *Candida albicans* as well as minimal effects against *Aspergillus sp.* The laboratory findings demonstrated that the efinaconazole NLC gel provides strong antifungal abilities which establish it as a promising option for topical antifungal treatment [43].

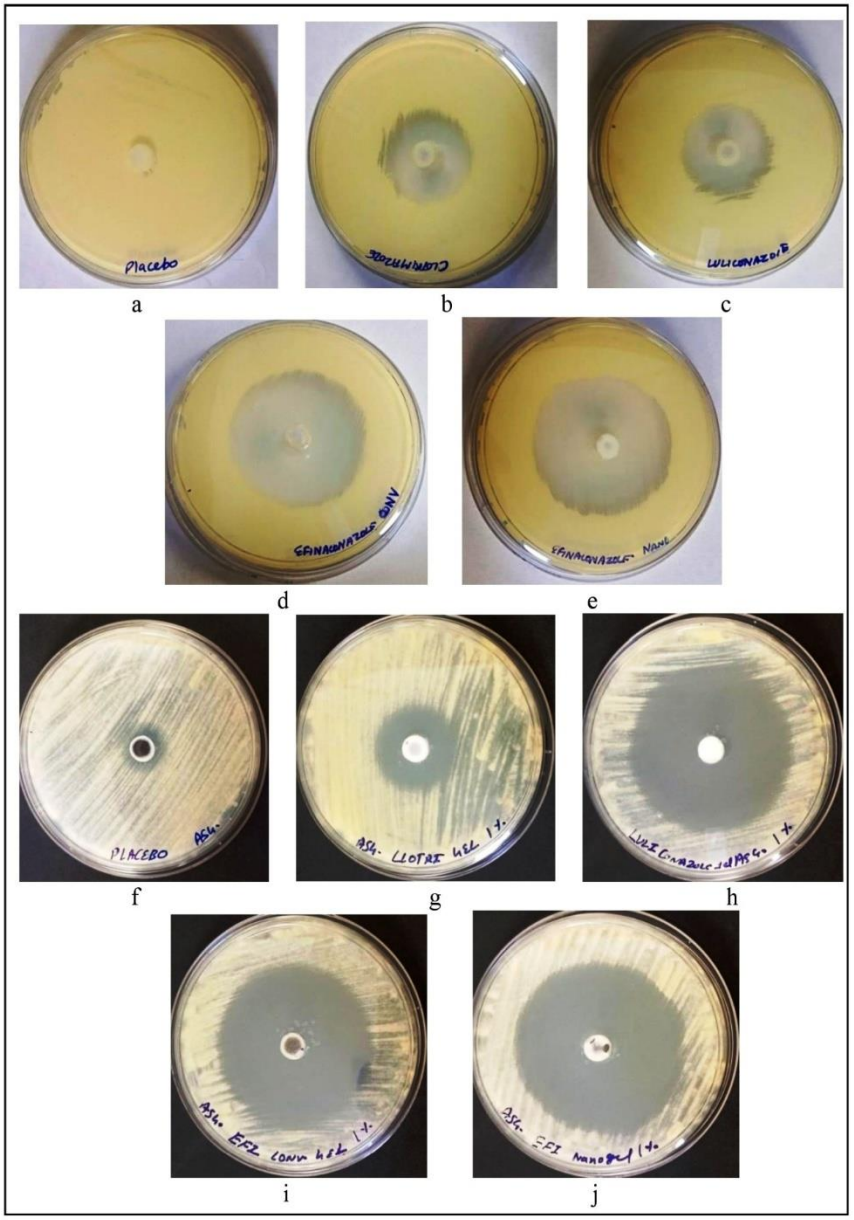

Fig. 12. Antifungal activity against *Candida albicans* for formulation (a) Placebo (b) clotrimazole gel 1% (c) luliconazole gel 1% (d) efinaconazole conventional gel 1% and (e) efinaconazole NLC gel 1%, and antifungal activity against *Aspergillus* Sp. for formulation (f) Placebo (g) clotrimazole gel 1% (h) luliconazole gel 1% (i) efinaconazole conventional gel 1% and (j) efinaconazole NLC gel 1%.

Stability Study

The testing of EFI-NLC gel stability was investigated under conditions of 25°C/60% RH and 40°C/75% RH for six months to assess pH behavior together with viscosity measurements, torque evaluation and drug content determination. The formulation components stayed undisturbed during the study period because the pH values demonstrated stable measurements between 6.63 and 6.79. The gel consistency decreased slightly from 85,200 cps at 1M-25°C/60% RH to 76,200 cps at 6M-40°C/75% RH during the storage period under accelerated conditions. The mechanical strength of gels experienced minimal changes based on torque measurements which reduced from 43.1 to 38.7. The drug content analysis revealed more than 98.95% throughout the study period establishing EFI-NLC stability without substantial drug loss based on data presented in table 8. The formulated product maintained excellent stability during standard and testing conditions for six months while displaying minimal physicochemical variations thus ensuring long-term product storage.

Table 8. Stability data of the EFI-NLC gel

S. No.	Condition	pH ± SD	Viscosity (cps) ± SD	Torque (%) ± SD	Drug Content (%) ± SD
1	1M-25°C/60%RH	6.75±0.04	85200±0.45	43.1±0.21	99.82±0.52
2	3M-25°C/60%RH	6.79±0.02	82800±0.52	41.5±0.12	100.12±0.32
3	6M-25°C/60%RH	6.71±0.05	84300±0.21	42.8±0.24	99.12±0.85
4	1M-40°C/75%RH	6.73±0.01	83700±0.15	42.2±0.13	100.21±0.31
5	3M-40°C/75%RH	6.68±0.03	80900±0.35	40.8±0.45	99.52±0.26
6	6M-40°C/75%RH	6.63±0.02	76200±0.75	38.7±0.25	98.95±0.96

SD: Standard Deviation

4. CONCLUSION

This study successfully developed and characterized efinaconazole-loaded nanostructured lipid carriers (EFI-NLCs) along with performant characterization for improving topical delivery and antifungal properties of efinaconazole through enhancing water solubility and skin penetration. The formulation process utilized glyceryl monostearate as solid lipid and propylene glycol monolaurate as liquid lipid with Tween 80 as stabilizer to produce NLC particles showing high encapsulation efficiency of 85% while maintaining nanometer-scale stability, which was confirmed by SEM and FTIR analysis. The diffractometric scanning curves confirmed a transition from crystalline to amorphous efinaconazole states through a liquid crystalline drug formulation, which showed a 122.61°C peak with decreased energy capacity at 35.49 J/g. The altered state of the drug, as confirmed by drug release tests, indicates better bioavailability and solubility. The formulation presented stable characteristics and low cytotoxicity with improved antifungal effects against *Candida albicans* and *Aspergillus* species. The reduction in fungal burdens, along with low systemic penetration and minimal side effects, highlights the potential of EFI-NLCs as an effective, safe, and targeted topical therapy for superficial fungal skin infections.

Author's contributions

A.K. contributed to manuscript writing, data collection and processing, literature search, figures and tables. A.S. contributed to the *in vitro* biological study and S.K. contributed to the concept, design, analysis of data, figures, and tables.

Acknowledgement

The authors are thankful to Vyome Therapeutics Limited, Delhi, Invictus Oncology Pvt Ltd, Delhi and School of Pharmaceutical Sciences, Om Sterling Global University, Hisar for providing the facilities & supported respectively for carried out the research work.

Funding

The author has no relevant financial or non-financial interest to disclose.

Conflicts of interest

The authors declare no competing interests.

Ethical Approval

As this study does not involve animal and patient experiments, the ethical approval and consent to participate are not applicable.

REFERENCES

[1] F. Almeida, M.L. Rodrigues, C. Coelho, The Still Underestimated Problem of Fungal Diseases Worldwide, Front. Microbiol.10 (2019) 214. https://doi.org/10.3389/fmicb.2019.00214.

[2] G.K.K. Reddy, A.R. Padmavathi, Y.V. Nancharaiah, Fungal infections: Pathogenesis, antifungals and alternate treatment approaches, Current Research in Microbial Sciences 3 (2022) 100137. https://doi.org/10.1016/j.crmicr.2022.100137.

[3] J.R. Kohler, A. Casadevall, J. Perfect, The Spectrum of Fungi That Infects Humans, Cold Spring Harbor Perspectives in Medicine 5 (2015) a019273–a019273. https://doi.org/10.1101/cshperspect.a019273.

[4] P. Chanyachailert, C. Leeyaphan, S. Bunyaratavej, Cutaneous Fungal Infections Caused by Dermatophytes and Non-Dermatophytes: An Updated Comprehensive Review of Epidemiology, Clinical Presentations, and Diagnostic Testing, JoF 9 (2023) 669. https://doi.org/10.3390/jof9060669.

[5] S.R. Jartarkar, A. Patil, Y. Goldust, C.J. Cockerell, R.A. Schwartz, S. Grabbe, M. Goldust, Pathogenesis, Immunology and Management of Dermatophytosis, JoF 8 (2021) 39. https://doi.org/10.3390/jof8010039.

[6] H.R. Mahmood, M. Shams-Ghahfarokhi, Z. Salehi, M. Razzaghi-Abyaneh, Epidemiological trends, antifungal drug susceptibility and SQLE point mutations in etiologic species of human dermatophytosis in Al-Diwaneyah, Iraq, Sci Rep 14 (2024) 12669. https://doi.org/10.1038/s41598-024-63425-w.

[7] J.A.M.S. Jayatilake, A Review of the Ultrastructural Features of Superficial Candidiasis, Mycopathologia 171 (2011) 235–250. https://doi.org/10.1007/s11046-010-9373-7.

[8] G. Teklebirhan, Profile of Dermatophyte and Non Dermatophyte Fungi in Patients Suspected of Dermatophytosis, AJLS 3 (2015) 352. https://doi.org/10.11648/j.ajls.20150305.13.

[9] Gesew, G. T. Prevalence of dermatophytes and non-dermatophyte fungal Infection among patients visiting dermatology clinic, at TikurAnbessa hospital (Addis Ababa, Ethiopia, Addis Ababa University, 2014).

[10] A.K. Gupta, T. Wang, E.A. Cooper, R.C. Summerbell, V. Piguet, A. Tosti, B.M. Piraccini, A comprehensive review of nondermatophytemould onychomycosis: Epidemiology, diagnosis and management, AcadDermatolVenereol 38 (2024) 480–495. https://doi.org/10.1111/jdv.19644.

[11] A. Arastehfar, T. Gabaldón, R. Garcia-Rubio, J.D. Jenks, M. Hoenigl, H.J.F. Salzer, M. Ilkit, C. Lass-Flörl, D.S. Perlin, Drug-Resistant Fungi: An Emerging Challenge Threatening Our Limited Antifungal Armamentarium, Antibiotics 9 (2020) 877. https://doi.org/10.3390/antibiotics9120877.

[12] K. Iozumi, M. Abe, Y. Ito, T. Uesugi, T. Onoduka, I. Kato, F. Kato, K. Kodama, H. Takahashi, O. Takeda, K. Tomizawa, T. Nomiyama, M. Fujii, J. Mayama, F. Muramoto, H. Yasuda, K. Yamanaka, T. Sato, T. Oh-i, H. Kasai, R. Tsuboi, N. Hattori, R. Maruyama, T. Omi, H. Shimoyama, Y. Sei, I. Nakasu, S. Nishimoto, Y. Hata, T. Mochizuki, M. Fukuzawa, M. Seishima, K. Sugiura, I. Katayama, O. Yamamoto, M. Shindo, H. Kiryu, M. Kusuhara, M. Takenaka, S. Watanabe, Efficacy of long-term treatment with efinaconazole 10% solution in patients with onychomycosis, including severe cases: A multicenter, single-arm study, The Journal of Dermatology 46 (2019) 641–651. https://doi.org/10.1111/1346-8138.14935.

[13] V. Bhatt, R. Pillai, Efinaconazole Topical Solution, 10%: Formulation Development Program of a New Topical Treatment of Toenail Onychomycosis, Journal of Pharmaceutical Sciences 104 (2015) 2177–2182. https://doi.org/10.1002/jps.24459.

[14] A.K. Gupta, F.C. Simpson, Efinaconazole (Jublia) for the treatment of onychomycosis, Expert Review of Anti-Infective Therapy 12 (2014) 743–752. https://doi.org/10.1586/14787210.2014.919852.

[15] C. Gorzelanny, C. Mess, S.W. Schneider, V. Huck, J.M. Brandner, Skin Barriers in Dermal Drug Delivery: Which Barriers Have to Be Overcome and How Can We Measure Them?, Pharmaceutics 12 (2020) 684. https://doi.org/10.3390/pharmaceutics12070684.

[16] S. Baghel, V.S. Nair, A. Pirani, A.B. Sravani, B. Bhemisetty, K. Ananthamurthy, J.M. Aranjani, S.A. Lewis, Luliconazole-loaded nanostructured lipid carriers for topical treatment of superficial Tinea infections, Dermatologic Therapy 33 (2020). https://doi.org/10.1111/dth.13959.

[17] B. Palmer, L. DeLouise, Nanoparticle-Enabled Transdermal Drug Delivery Systems for Enhanced Dose Control and Tissue Targeting, Molecules 21 (2016) 1719. https://doi.org/10.3390/molecules21121719.

[18] Y.-Q. Yu, X. Yang, X.-F.Wu, Y.-B. Fan, Enhancing Permeation of Drug Molecules Across the Skin via Delivery in Nanocarriers: Novel Strategies for Effective Transdermal Applications, Front. Bioeng.Biotechnol.9 (2021) 646554. https://doi.org/10.3389/fbioe.2021.646554.

[19] S.Z. Alshawwa, A.A. Kassem, R.M. Farid, S.K. Mostafa, G.S. Labib, Nanocarrier Drug Delivery Systems: Characterization, Limitations, Future Perspectives and Implementation of Artificial Intelligence, Pharmaceutics

14 (2022) 883. https://doi.org/10.3390/pharmaceutics14040883.

[20] P. Ghasemiyeh, S. Mohammadi-Samani, Potential of Nanoparticles as Permeation Enhancers and Targeted Delivery Options for Skin: Advantages and Disadvantages, DDDT Volume 14 (2020) 3271–3289. https://doi.org/10.2147/DDDT.S264648.

[21] S. Gupta, P. Kumar, Drug Delivery Using Nanocarriers: Indian Perspective, Proc. Natl. Acad. Sci., India, Sect. B Biol. Sci. 82 (2012) 167–206. https://doi.org/10.1007/s40011-012-0080-7.

[22] C.M.B. Pinilla, N.A. Lopes, A. Brandelli, Lipid-Based Nanostructures for the Delivery of Natural Antimicrobials, Molecules 26 (2021) 3587. https://doi.org/10.3390/molecules26123587.

[23] S. Nene, S. Shah, N. Rangaraj, N.K. Mehra, P.K. Singh, S. Srivastava, Lipid based nanocarriers: A novel paradigm for topical antifungal therapy, Journal of Drug Delivery Science and Technology 62 (2021) 102397. https://doi.org/10.1016/j.jddst.2021.102397.

[24] M. Haider, S.M. Abdin, L. Kamal, G. Orive, Nanostructured Lipid Carriers for Delivery of Chemotherapeutics: A Review, Pharmaceutics 12 (2020) 288. https://doi.org/10.3390/pharmaceutics12030288.

[25] E.A. Madawi, A.R. Al Jayoush, M. Rawas-Qalaji, H.E. Thu, S. Khan, M. Sohail, A. Mahmood, Z. Hussain, Polymeric Nanoparticles as Tunable Nanocarriers for Targeted Delivery of Drugs to Skin Tissues for Treatment of Topical Skin Diseases, Pharmaceutics 15 (2023) 657. https://doi.org/10.3390/pharmaceutics15020657.

[26] Talei, M. R. Metal nanoparticles as Novel Drug Delivery systems: a review of current challenges and opportunities. Iraqi J. Nat. Sci. Nanatechnol. 4 (2023) 113–140.

[27] J.K. Patra, G. Das, L.F. Fraceto, E.V.R. Campos, M.D.P. Rodriguez-Torres, L.S. Acosta-Torres, L.A. Diaz-Torres, R. Grillo, M.K. Swamy, S. Sharma, S. Habtemariam, H.-S. Shin, Nano based drug delivery systems: recent developments and future prospects, J Nanobiotechnol 16 (2018) 71. https://doi.org/10.1186/s12951-018-0392-8.

[28] N.M. Mahajan, ed., Photophysics and nanophysics in therapeutics, Elsevier, Amsterdam, Netherlands, 2022.

[29] M. Elmowafy, M.M. Al-Sanea, Nanostructured lipid carriers (NLCs) as drug delivery platform: Advances in formulation and delivery strategies, Saudi Pharmaceutical Journal 29 (2021) 999–1012. https://doi.org/10.1016/j.jsps.2021.07.015.

[30] A. Khosa, S. Reddi, R.N. Saha, Nanostructured lipid carriers for site-specific drug delivery, Biomedicine & Pharmacotherapy 103 (2018) 598–613. https://doi.org/10.1016/j.biopha.2018.04.055.

[31] S. Khan, A. Sharma, V. Jain, An Overview of Nanostructured Lipid Carriers and its Application in Drug Delivery through Different Routes, Adv Pharm Bull 13 (2023) 446–460. https://doi.org/10.34172/apb.2023.056.

[32] S. Babaei, S. Ghanbarzadeh, Z.M. Adib, M. Kouhsoltani, S. Davaran, H. Hamishehkar, Enhanced skin penetration of lidocaine through encapsulation into nanoethosomes and nanostructured lipid carriers: a comparative study, Pharmazie 71 (2016) 247–251.

[33] B. Gaba, M. Fazil, S. Khan, A. Ali, S. Baboota, J. Ali, Nanostructured lipid carrier system for topical delivery of terbinafine hydrochloride, Bulletin of Faculty of Pharmacy, Cairo University 53 (2015) 147–159. https://doi.org/10.1016/j.bfopcu.2015.10.001.

[34] Ma Jia Yuan, HashamRosnani, AbdRasidZaitulIffa, Mohamed Noor Norhayati, Formulation and Characterization of Nanostructured Lipid Carrier Encapsulate Lemongrass Oil Using Ultrasonication Technique, Chemical Engineering Transactions 83 (2021) 475–480. https://doi.org/10.3303/CET2183080.

[35] M. Saeedi, K. Morteza-Semnani, A. Siahposht-Khachaki, J. Akbari, M. Valizadeh, A. Sanaee, B. Jafarkhani, M. Eghbali, H.H.H. Zanjani, S.M.H. Hashemi, S.M. Rahimnia, Passive Targeted Drug Delivery of Venlafaxine HCl to the Brain by Modified Chitosan Nanoparticles: Characterization, Cellular Safety Assessment, and In Vivo Evaluation, J Pharm Innov 18 (2023) 1441–1453. https://doi.org/10.1007/s12247-023-09733-6.

[36] E.S. Behbahani, M. Ghaedi, M. Abbaspour, K. Rostamizadeh, Optimization and characterization of ultrasound assisted preparation of curcumin-loaded solid lipid nanoparticles: Application of central composite design, thermal analysis and X-ray diffraction techniques, UltrasonicsSonochemistry 38 (2017) 271–280. https://doi.org/10.1016/j.ultsonch.2017.03.013.

[37] E. Taha, S.A. Nour, W. Mamdouh, A.A. Selim, M.M. Swidan, A.B. Ibrahim, M.J. Naguib, Cod liver oil nano-structured lipid carriers (Cod-NLCs) as a promising platform for nose to brain delivery: Preparation, in vitro optimization, ex vivo cytotoxicity & in vivo biodistribution utilizing radioiodinatedzopiclone, International Journal of Pharmaceutics: X 5 (2023) 100160. https://doi.org/10.1016/j.ijpx.2023.100160.

[38] A. Vikas, P. Rashmin, P. Mrunali, M. Sandip, T. Kaushik, RP-HPLC method for quantitative estimation of

Efinaconazole in topical microemulsion and microemulsion-based-gel formulations and in presence of its degradation products, Microchemical Journal 155 (2020) 104753. https://doi.org/10.1016/j.microc.2020.104753.

[39] N.K. Garg, N. Tandel, S.K. Bhadada, R.K. Tyagi, Nanostructured Lipid Carrier–Mediated Transdermal Delivery of Aceclofenac Hydrogel Present an Effective Therapeutic Approach for Inflammatory Diseases, Front. Pharmacol.12 (2021) 713616. https://doi.org/10.3389/fphar.2021.713616.

[40] S. Kalepu, M. Manthina, V. Padavala, Oral lipid-based drug delivery systems – an overview, ActaPharmaceuticaSinica B 3 (2013) 361–372. https://doi.org/10.1016/j.apsb.2013.10.001.

[41] A.C. Silva, E. González-Mira, M.L. García, M.A. Egea, J. Fonseca, R. Silva, D. Santos, E.B. Souto, D. Ferreira, Preparation, characterization and biocompatibility studies on risperidone-loaded solid lipid nanoparticles (SLN): High pressure homogenization versus ultrasound, Colloids and Surfaces B: Biointerfaces 86 (2011) 158–165. https://doi.org/10.1016/j.colsurfb.2011.03.035.

[42] S. Das, A.B.H. Wong, Stabilization of ferulic acid in topical gel formulation via nanoencapsulation and pH optimization, Sci Rep 10 (2020) 12288. https://doi.org/10.1038/s41598-020-68732-6.

[43] V. Agrawal, R. Patel, M. Patel, K. Thanki, S. Mishra, Design and evaluation of microemulsion-based efinaconazole formulations for targeted treatment of onychomycosis through transungual route: Ex vivo and nail clipping studies, Colloids and Surfaces B: Biointerfaces 201 (2021) 111652. https://doi.org/10.1016/j.colsurfb.2021.111652.

[44] S.S. Patil, P. Khulbe, M.M. Nitalikar, K. Das, M. B.P., S. Alshehri, A.M.S. Khormi, M.E.M. Almalki, S.A. Hussain, S.I. Rabbani, S.M.B. Asdaq, Development of topical silver nano gel formulation of Bixin: Characterization, and evaluation of anticancer activity, Saudi Pharmaceutical Journal 32 (2024) 102125. https://doi.org/10.1016/j.jsps.2024.102125.

[45] A. Ahad, Mohd. Aqil, A. Ali, Investigation of antihypertensive activity of carbopol valsartan transdermal gel containing 1,8-cineole, International Journal of Biological Macromolecules 64 (2014) 144–149. https://doi.org/10.1016/j.ijbiomac.2013.11.018.

[46] Y. Bachhav, V. Patravale, Microemulsion based vaginal gel of fluconazole: Formulation, in vitro and in vivo evaluation, International Journal of Pharmaceutics 365 (2009) 175–179. https://doi.org/10.1016/j.ijpharm.2008.08.021.

[47] Indian Pharmacopoeia, 4.2. General Reagents 1 (2022) 563.

[48] F. Han, R. Yin, X. Che, J. Yuan, Y. Cui, H. Yin, S. Li, Nanostructured lipid carriers (NLC) based topical gel of flurbiprofen: Design, characterization and in vivo evaluation, International Journal of Pharmaceutics 439 (2012) 349–357. https://doi.org/10.1016/j.ijpharm.2012.08.040.

[49] S.K. Sadozai, S.A. Khan, A. Baseer, R. Ullah, A. Zeb, M. Schneider, In Vitro, Ex Vivo, and In Vivo Evaluation of Nanoparticle-Based Topical Formulation Against Candida albicans Infection, Front. Pharmacol.13 (2022) 909851. https://doi.org/10.3389/fphar.2022.909851.

[50] E. Sieniawska, Ł. Świątek, M. Wota, B. Rajtar, M. Polz-Dacewicz, Microemulsions of essentials oils – Increase of solubility and antioxidant activity or cytotoxicity?, Food and Chemical Toxicology 129 (2019) 115–124. https://doi.org/10.1016/j.fct.2019.04.038.

[51] H. Kansagra, S. Mallick, Microemulsion-based antifungal gel of luliconazole for dermatophyte infections: formulation, characterization and efficacy studies, Journal of Pharmaceutical Investigation 46 (2016) 21–28. https://doi.org/10.1007/s40005-015-0209-9.

[52] K. Krambeck, V. Silva, R. Silva, C. Fernandes, F. Cagide, F. Borges, D. Santos, F. Otero-Espinar, J.M.S. Lobo, M.H. Amaral, Design and characterization of Nanostructured lipid carriers (NLC) and Nanostructured lipid carrier-based hydrogels containing Passifloraedulis seeds oil, International Journal of Pharmaceutics 600 (2021) 120444. https://doi.org/10.1016/j.ijpharm.2021.120444.

[53] E.B. Souto, S.A. Wissing, C.M. Barbosa, R.H. Müller, Development of a controlled release formulation based on SLN and NLC for topical clotrimazole delivery, International Journal of Pharmaceutics 278 (2004) 71–77. https://doi.org/10.1016/j.ijpharm.2004.02.032.

[54] E. Esposito, M. Drechsler, R. Cortesi, C. Nastruzzi, Encapsulation of cannabinoid drugs in nanostructured lipid carriers, European Journal of Pharmaceutics and Biopharmaceutics 102 (2016) 87–91. https://doi.org/10.1016/j.ejpb.2016.03.005.

[55] M. Nosratabadi, S.M. Rahimnia, R.E. Barogh, M. Abastabar, I. Haghani, J. Akhtari, Z. Hajheydari, P. Ebrahimnejad, Luliconazole-loaded nanostructured lipid carrier: formulation, characterization, and in vitro antifungal evaluation against a panel of resistant fungal strains, Sci Rep 14 (2024) 30708.

https://doi.org/10.1038/s41598-024-79225-1.

[56] S.R. Castro, L.N.M. Ribeiro, M.C. Breitkreitz, V.A. Guilherme, G.H. Rodrigues Da Silva, H. Mitsutake, A.C.S. Alcântara, F. Yokaichiya, M.K.K.D. Franco, D. Clemens, B. Kent, M. Lancellotti, D.R. De Araújo, E. De Paula, A pre-formulation study of tetracaine loaded in optimized nanostructured lipid carriers, Sci Rep 11 (2021) 21463. https://doi.org/10.1038/s41598-021-99743-6.

[57] A.B. Nair, B. Aldhubiab, J. Shah, S. Jacob, M. Attimarad, N. Sreeharsha, K.N. Venugopala, A. Joseph, M.A. Morsy, Design, Development, and Evaluation of Constant Voltage Iontophoresis for the Transungual Delivery of Efinaconazole, Pharmaceutics 15 (2023) 1422. https://doi.org/10.3390/pharmaceutics15051422.

[58] Shamim, T. Ali, Chromatography and Spectroscopic Technique-Based Rapid Characterization of Nano-Carrier Pharmaceuticals, PNT 13 (2024). https://doi.org/10.2174/0122117385319695240911115239.

[59] P. Borah, S. Hazarika, D. Sharma, K.N. Venugopala, D. Chopra, N.A. Al-Shar'i, S. Hemalatha, A.K. Shakya, P. Chandra Acharya, P.K. Deb, Systemic and topical antifungal drugs, in: Medicinal Chemistry of Chemotherapeutic Agents, Elsevier, 2023: pp. 285–315. https://doi.org/10.1016/B978-0-323-90575-6.00002-8.

[60] sandrawati, In vitro cytotoxic activity assay of bacteria extract derived marine sponge Haliclonafascigera toward Hela, WiDr, T47D, and Vero cell line, J App Pharm Sci 9 (2019) 66–70. https://doi.org/10.7324/JAPS.2019.90809.

[61] P. Mittal, M. Singla, Smriti, R. Kapoor, D. Kumar, S. Gupta, G. Gupta, T. Bhattacharya, Paclitaxel loaded Capmul MCM and tristearin based nanostructured lipid carriers (NLCs) for glioblastoma treatment: screening of formulation components by quality by design (QbD) approach, Discover Nano 19 (2024) 175. https://doi.org/10.1186/s11671-024-04132-3.

[62] C. Comby-Zerbino, X. Dagany, F. Chirot, P. Dugourd, R. Antoine, The emergence of mass spectrometry for characterizing nanomaterials. Atomically precise nanoclusters and beyond, Mater. Adv. 2 (2021) 4896–4913. https://doi.org/10.1039/D1MA00261A.

[63] R. Aggarwal, M. Targhotra, P.K. Sahoo, M.K. Chauhan, Efinaconazole nail lacquer for the transungual drug delivery: Formulation, optimization, characterization and in vitro evaluation, Journal of Drug Delivery Science and Technology 60 (2020) 101998. https://doi.org/10.1016/j.jddst.2020.101998.

[64] C. Khot, K. Kolekar, S. Dabhole, A. Mohite, S. Nadaf, P.S. Kumbhar, J. Disouza, Optimized albendazole-loaded nanostructured lipid carrier gel: a redefined approach for localized skin cancer treatment, RSC Pharm. 1 (2024) 1042–1054. https://doi.org/10.1039/D4PM00207E.

[65] K. A, S. Sk, D. M, K. R, Y. Ak, K. V, C. H, Development and Validation of Liquid Chromatography (RP-HPLC) Methodology for Estimation of EfonidipineHClEthanolate (EFD), Pharm Anal Acta 08 (2017). https://doi.org/10.4172/2153-2435.1000547.

[66] A. Kumar, P. Saharan, S. Kumar, Eco-friendly RP-HPLC method development and validation for simultaneous determination of triazole antifungal agent and benzyl alcohol in nanostructured lipid carrier-based bulk and gel formulations, J Neonatal Surg 14 (2025) 757–777. https://jneonatalsurg.com/index.php/jns/article/view/2951.

[67] S. Brito Raj, K.B. Chandrasekhar, K.B. Reddy, Formulation, in-vitro and in-vivo pharmacokinetic evaluation of simvastatin nanostructured lipid carrier loaded transdermal drug delivery system, Futur J Pharm Sci 5 (2019) 9. https://doi.org/10.1186/s43094-019-0008-7.

[68] D. Verma, P.S. Thakur, S. Padhi, T. Khuroo, S. Talegaonkar, Z. Iqbal, Design expert assisted nanoformulation design for co-delivery of topotecan and thymoquinone: Optimization, in vitro characterization and stability assessment, Journal of Molecular Liquids 242 (2017) 382–394. https://doi.org/10.1016/j.molliq.2017.07.002.

[69] T. Alam, Quality by design based development of nanostructured lipid carrier: a risk based approach, Exploration of Medicine (2022) 617–638. https://doi.org/10.37349/emed.2022.00118.

[70] S. Bhattacharya, Central Composite Design for Response Surface Methodology and Its Application in Pharmacy, in: P. Kayaroganam (Ed.), Response Surface Methodology in Engineering Science, IntechOpen, 2021. https://doi.org/10.5772/intechopen.95835.

[71] H. Hassan, S.K. Adam, E. Alias, M.M.R. MeorMohdAffandi, A.F. Shamsuddin, R. Basir, Central Composite Design for Formulation and Optimization of Solid Lipid Nanoparticles to Enhance Oral Bioavailability of Acyclovir, Molecules 26 (2021) 5432. https://doi.org/10.3390/molecules26185432.